Acta Scientific Pharmaceutical Sciences

Volume 2 Issue 2 February 2018

Research Article

Characterization and Predictive QSAR Analysis of Azasteroids as Five Alpha Reductase Inhibitors

Richa, Meenakshi Sharma, Monika, Renu Chadha and Neelima Dhingra*

Department of Pharmaceutical Chemistry, University Institute of Pharmaceutical Sciences, Panjab University, Chandigarh, India

***Corresponding Author:** Neelima Dhingra, Assistant Professor Department of Pharmaceutical Chemistry, University Institute of Pharmaceutical Sciences, Panjab University, Chandigarh, India.

Received: December 27, 2017; **Published:** January 18, 2018

Graphical Abstract

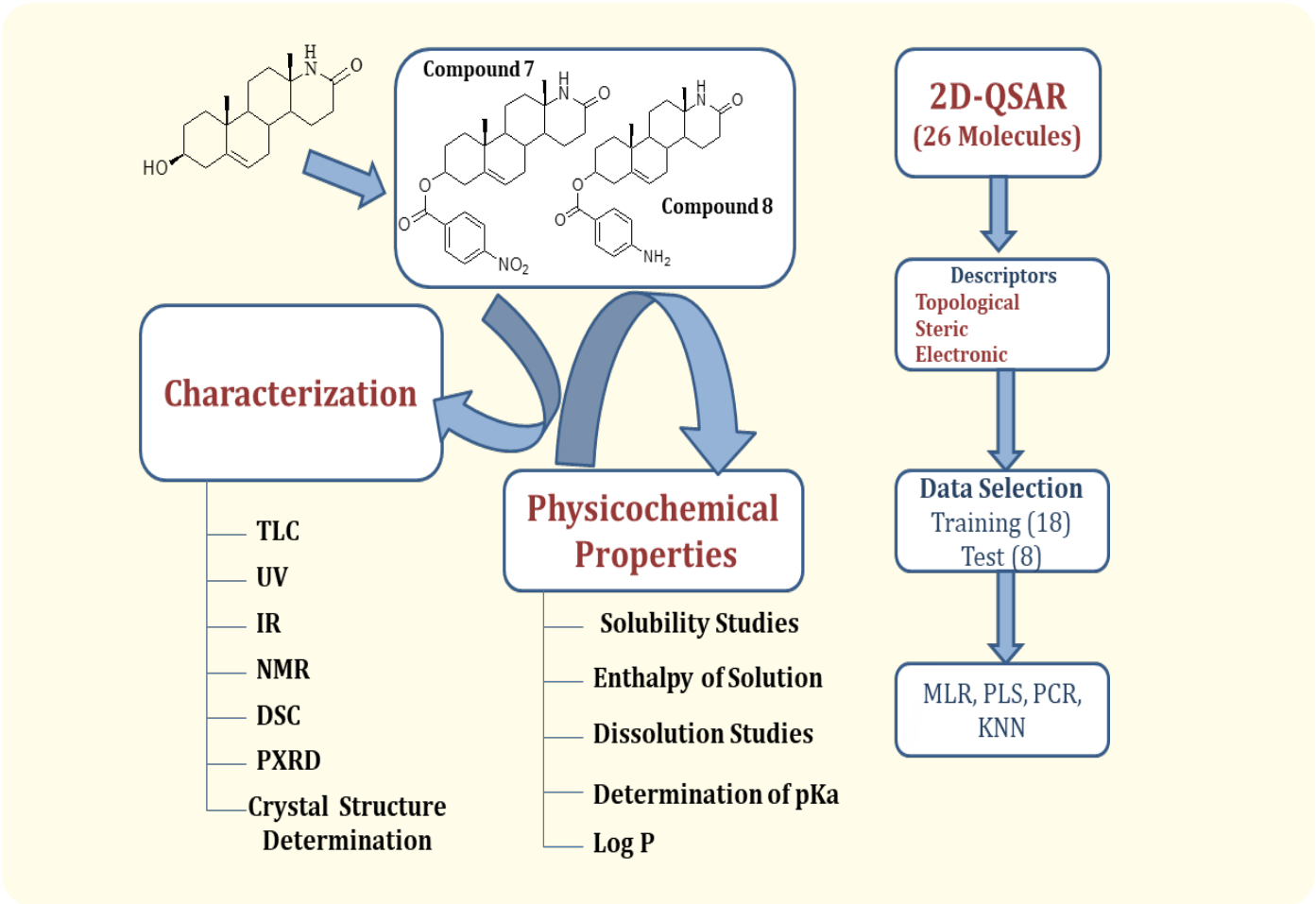

Abstract

Background and Objective: Major circulating hormone dihydrotestosterone (DHT) is responsible for the development and progression of benign prostate hyperplasia (BPH). The enzyme 5α-reductase (5alpha R) catalyses the reduction of testosterone (T) into the more potent androgen dihydrotestosterone (DHT). Inhibition of 5α-Reductase enzyme is the novel approach for treatment of BPH.

Method: Present work describes synthesis of 17-Oxo-17a-aza-D-homo-5-androsten-3β-yl 4-nitrobenzoate **(7)**, 17-oxo-17a-aza-d-homo-5-androsten-3β-yl 4-aminobenzoate **(8)** as 5α-reductase inhibitors and their structural characterization using spectral, DSC and PXRD techniques. Preliminary physicochemical properties solubility, dissolution rates, pKa and permeability (log P) has also been determined.

Conclusion: The statistically validated two-dimensional quantitative structure activity relationship (2D QSAR) model was obtained using structurally related 3β-substituted esters of 17a-Aza, 17-oximino, 17-oxo androstane derivatives, through partial least squares (PLS) analysis method of stepwise forward-backward approach. Statistical data of Model 1 (r^2 = 0.833, q^2 = 0.671; F = 37.498, pred r^2 = 0.736) correlated with human 5α-reductase inhibitory activity. Validation was done with LOO method. Four descriptors showing positive and negative correlation with the 5α-Reductase inhibitory activity have been included in the model. Physicochemical characterization and statistically correlated model with 5α-reductase activity has not only added to the bank information of the synthesized highly significant molecules, but has also provided a overview of their bioperformance, and facilitated decision making during lead optimization.

Keywords: BPH; 5α-Reductase Inhibitors; Steroidal lactams; DSC; Log P; 2D-QSAR

Abbreviations

BPH: Benign Prostate Hyperplasia; DHT: Dihydrotestosterone; GA: Genetic Algorithmic; MDS: Molecular Design Suits; MLR: Multiple Linear Regressions; PCR: Principal Component Regression; PLS: Partial Least Squares; SA: Simulated Annealing; SE: Sphere Exclusion; SW-F: Stepwise Forward; SW-FB: Stepwise Forward-Backward; T: Testosterone; QSAR: Quantitative Structure Activity Relationship

Introduction

Benign prostatic hyperplasia (BPH) is a general term for the non-cancerous growth of prostate gland with the increase in number of epithelial and stromal cells. The of BPH increases with increasing age and approximately 40 and 80% of men have been found to be affected with moderate to severe symptoms at the age of 60 and 80 years, respectively. Nearly all men develop microscopic BPH by the age of 90 years [1].

Clinically it is manifested as lower urinary tract symptoms (LUTS) consisting of irritative (urgency, nocturia, frequency,) and obstructive symptoms (hesitancy, a sensation of incomplete bladder emptying, a weak and interrupted urinary stream, straining to initiate urination,) [2,3]. Androgen signalling cascade involves the synthesis and release of testosterone (T) **(1)** in testes and adrenal glands, which gets peripherally converted to dihydrotestosterone (DHT) **(2)** under the effect of membrane bound NADPH dependent 5α-reductase enzyme and is shown in figure 1 [4, 5]. Two different isoforms of 5α-reductase enzyme type 1 and type II have been isolated and characterized and they differ in term of their location, sequence of amino acids, molecular weight range of pH for their optimal activity and biological effects [6-9]. DHT once formed, get circulated to the target tissues where it binds with target androgen receptors (AR). Both T and DHT bind to and activate the AR, but DHT has been found to bound with a greater affinity thus leading to different kinetic processes [10-13]. Thus 5α-reductase dictates the cellular availability of DHT to prostatic epithelial cells and consequently modulates its growth [14-16]. The raised levels of DHT cause pathological conditions like acne [16] hirsutism [17-19] androgenic alopecia [20,21] and BPH [22-24]. Inhibitors of androgen action by 5α-reductase, founds to be a logical treatment for the benign prostate hyperplasia. These agents by blocking the enzyme suppress the DHT concentration, helps in shrinking the size of prostate and ultimately provide relief from the symptoms related to the static and mechanical obstruction caused by BPH.

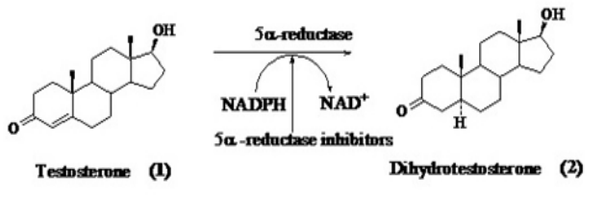

Figure 1: Conversion of testosterone into Dihydrotestosterone.

During past two decades several steroidal and non-steroidal compounds have been synthesized and reported from competitive to non-competitive or reversible to irreversible 5α-reductase inhibitors [25-28], Steroidal compounds represented the major attention due to their lipophilic character and remarkable progress has been made in the designing and synthesis of these inhibitors by modifying the different positions of basic steroidal nucleus with various substitutions. Diversified chemical classes like carboxysteroids [29], 6-azasteroids [30], 11-azasteroids [31], 19-Nor-10-azasteroids [32], 15- and 16-Azasteroids [33] and 4-azasreroids [34] have been reported to possess *in vitro* and *in vivo* 5α-reductase inhibitory potency. Of these, 4-aza steroids were found to possess comparatively high inhibitory activity as exemplified by Finasteride [35] (MK-906), the first clinically approved 5 -reductase inhibitor for the treatment of BPH in 1992 (Figure 2a). MK-906 demonstrated its biochemical efficacy with an 80% reduction of intraprostatic DHT and 28% reduction in prostate size in patients with BPH [36]. A range of other 17–substituted 4-azasteroids were also studied for 5 -reductase inhibitory activity, led to the development of a new dual inhibitor Dutasteride in 2002 [29,37-39] (Figure 2a), by Glaxo Smith Kline, with the capability to reduce the dihydrotestosterone level by 85% [40-45]. The inhibitory activity of these azasteroids has been considered and attributed to the lactam in ring A of the steroidal nucleus that mimics intermediate transition state [46]. Various progesterone esters (Figure2b), have also shown high antiandrogenic activity [47] because they inhibit the enzymatic activity irreversibly, by forming a covalent linkage with the enzyme using their ester moiety. These observations led us to synthesize steroidal 5α-reductase inhibitors with lactam in ring D instead of ring A and ester moiety at position 3 of steroidal nucleus to have synergistic effect. Our previous published reports has indicated the synthesis of the compound 7 and 8 [48] along with % growth inhibition of the prostate cancer cell lines DU-145 88.89 ± 1.51 and 82.41 ± 2.69 respectively for during *in vitro* antiproliferative activity [48].

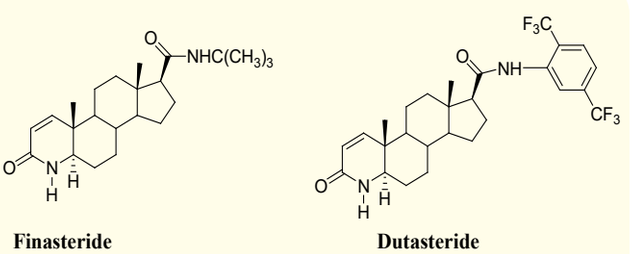

Figure 2a: Finasteride and Dutasteride.

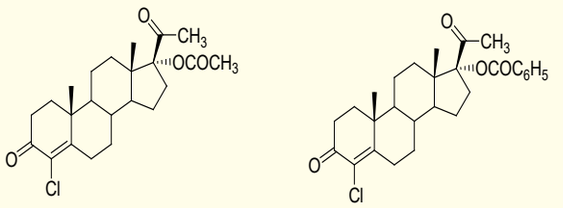

Figure 2b: Progesterone Esters.

One of the key challenges for Pharmaceutical Industry is to develop a pharmaceutical active ingredient with biological activity and appropriate physiochemical profile [49]. The properties that deals with physical and chemical characteristics of substance or drug molecule and helps in knowing about its transportation in body, distribution through different compartments, metabolism in the liver and other organs [50,51] are called physicochemical

properties. Drug molecules on interaction with biological receptor produces drug effect, and is preceded by drug transport from site of application to site of action, which purely depends on these properties ranging from molecular formula, molecular weight, melting or boiling point, particle size, stability studies, partition coefficient, solubility, dissolution, ionization constant or pka, enthalpy of solution, intermolecular forces, stereochemistry affecting pharmacokinetics [30,43]. Understanding of these physicochemical properties and integration of this knowledge with the absorption, intestinal permeability and metabolism (ADME biopharmaceutical) properties makes the formulation a rational and streamlined process and helps in choosing the optimal compounds from the task [44,52]. Further by alteration and optimization of these, not only we can improve the ADME of a chemical series in a chemotype-dependent manner, but it would save cost and time also [39,53].

Further, from past few years computer aided drug designing tool based on quantitative structure activity relationship (QSAR) has been used to increase the efficiency of the drug discovery process [54]. QSAR is a mathematical equation that integrate the relationship between biological activity of a molecular system and its geometric and chemical characteristics and these "rules" could be used to evaluate the activity of new compounds. In case of 5α-reductase enzyme, there is an immense interest in ligand based QSAR studies due to the lack of X-ray crystallography structure of target human enzyme. To further optimize the molecular architecture, we applied the linear free energy related (LFER) approach of Hansch [55] on a series of ester derivatives of 17a-azasteroidal, 17-oxo, 17-oximino androstane derivatives [48,56]. It will further help in rationalizing the physicochemical properties required in a molecule to develop new and effective inhibitors.

Material and Method

Experimental

The melting points were determined on Veego point melting apparatus and are uncorrected. Proton (1H-NMR) spectra were obtained using Brucker AC-300F, 300 MHz and Brucker AC 400F,400MHz spectrometer for solutions in deuteriochloroform, deuterated dimethyl sulfoxide and are reported in parts per million (ppm), downfield from tetramethylsilane (TMS) as internal standard. The spin multiplicities are indicated by the symbols, s (singlet), d (doublet), t (triplet), q (quartet), m (multiplet) and br (broad). Infrared (IR) spectra were obtained with Perkin Elmer 882 Spectrum and RXI, FT-IR model using a potassium bromide pellets (in cm^{-1}). The ultraviolet spectra were recorded on Perkin-Elmer, Lambda 35 spectrophotometer. Reactions were monitored and the homogeneity of the products was checked by TLC. Plates for thin layer chromatography (TLC) were prepared with silica gel G and activated at 110º for 30 minutes. Silica gel G60 F aluminum sheets plates were used for final monitoring. The plates were developed by exposure to iodine vapour. Anhydrous sodium sulphate was utilized as drying agents. All the solvents were dried and freshly distilled prior to use according to standard procedure.

General procedure for synthesis of substituted esters (7, 8) of 17-oxo-17a-aza-d-homo-5-androsten-3β-yl

To a stirred solution of 3β -hydroxy-17a-aza-D-homo-5-androsten-17-one (6) (0.5 g, 1.6 mmol) and dicyclohexylcarbodiimide (DCC) (0.34 g, 1.6 mmol) in anhydrous dichloromethane (30.0 mL) was added acid (1.6 mmol) and the mixture was stirred for 48h at room temperature. Disappearance of the starting material and completion of the reaction were confirmed by TLC. The precipitated dicyclohexylurea (DCU) was filtered and solvent removed under vacuum. The resulting residue was crystallized from ethyl acetate: petroleum ether (60:80).

17-oxo-17a-aza-d-homo-5-androsten-3β-yl 4-nitrobenzoate (7)

17-Oxo-17a-aza-D-homo-5-androsten-3β-yl 4-nitrobenzoate **(7)** (0.75 g, 75%), was prepared by method as described above using 4-nitrobenzoic acid (0.27g, 1.6 mmol) [48]. M.p. 206.33 ºC. R_f = 0.57, ($CHCl_3$: Methanol = 9.5 : 0.5); IR (KBr): 3298, 2931, 1698, 1650, and 1236 cm^{-1}; ^1H NMR ($CDCl_3$): δ 1.07 (s, 3H, 18-CH_3), 1.82 (s, 3H, 19-CH_3), 4.02 (m, 1H, 3α-H), 5.29 (br, s, 1H, 6-vinylic), 6.11 (1H, NH), 7.71 (d, 2H, 3-CH and 5-CH aromatic) and 8.28 ppm (d, 2H, 2-CH and 6-CH aromatic); Mass (ESI): 453.51 $[M+1]^+$; UV_{max} (Phosphate buffer 7.4): λ_{max} = 269.0 nm; $E^{1\%}_{1cm}$ = 491.45.

17-oxo-17a-aza-d-homo-5-androsten-3β-yl 4-aminobenzoate (8)

17-Oxo-17a-aza-D-homo-5-androsten-3β-yl 4-aminobenzoate **(8)** (0.50 g, 50%), was prepared by method as described above using 4-aminobenzoic acid (0.22g, 1.6 mmol) [48]. m.p. 188.37ºC. R_f = 0.61, ($CHCl_3$: Methanol = 9.6 : 0.4); IR (KBr): 3375, 3244, 2931, 1706, 1611 and 1239 cm^{-1}; ^1H NMR ($CDCl_3$): δ 1.10 (s, 3H, 18-CH_3), 1.49 (s, 3H, 19-CH_3), 4.15 (m, 1H, 3α-H), 5.42 (br, s, 1H, 6-vinylic), 5.93 (1H, NH), 6.62 (d, 2H, 3-CH and 5-CH aromatic), 7.44 (d, 2H, 2-CH and 6-CH aromatic) and 3.96 (s, 2H, br, NH_2 peak); Mass (ESI): 422.51 $[M]^+$; UV_{max} (Phosphate buffer 7.4): λ_{max} =276.0 nm; $E^{1\%}_{1cm}$ = 153.

Characterization

Differential Scanning Calorimetry (DSC)

DSC study of compound **7** and **8** were performed on DSC, Q20, TA-Instruments Waters (LLC, USA), calibrated with Indium. The samples were sealed in aluminum pan [57] and scanned with a heating rate of 10°C/min in the temperature range 25 - 250°C, under a dry nitrogen atmosphere (flow rate 50 cc/min). The results were integrated by TA Q series Advantage software (Universal analysis 2000).

Powder X-ray diffraction (PXRD)

Powder diffraction patterns of compound 7 and 8 were recorded on an X-ray diffractometer (X'PERT-PRO, Netherlands, Holand) with Cu as tube anode. The diffractograms were recorded under following conditions: voltage 45 kV, 40 mA, angular range 5, fixed divergence slit. The PXRD were analysed by X'PERT high Score software.

Crystal structure determination using material studio

The crystal structure of newly synthesized compounds were determined on Reflex Plus module of Material Studio using powder diffraction data. The overall prediction process was carried out in four steps; indexing, pawley fitting, structure solution and Rietveld refinement. In the indexing step, the crystal class and the approximate lattice parameters were derived from the peak positions in the experimental powder diffraction pattern using X-cell. A table was generated from the results of X-cell, that arrange the proposed unit cells according to their Figure of merit. Further an empty unit cell was generated based on the unit cell with the highest Figure of merit. The accurate lattice constants and the cell parameters were determined by Pawley fitting/refinement. The R_{wp} (weighted Rietveld parameter) value obtained after the refinement was used to establish the agreement between the calculated and the experimental powder patterns and hence confirmed the accuracy of the crystal class and the lattice parameters. The space group that showed the highest Figure of merit was selected and the pawley refinement was repeated with the selected space group to obtain another R_{wp}. The optimized structure of drug molecule was imported into the refined unit cell and motion groups were defined. The structure was obtained using the reflex powder solve that involved Monte Carlo/simulated annealing procedure. 10 Cycles of simulated annealing were selected with each cycle involving 2140100 number of steps. The similarity between the experimental and calculated diffraction patterns was confirmed by R_{wp} values. Further, Rietveld refinement of the structure solution was performed to obtain a final structure solution and a final R_{wp} value.

Physicochemical Properties

Solubility Studies

The solubility studies of synthesized compounds **7, 8** and standard drug Finasteride were performed by dissolving an excess amount of drug (approximately 20 mg) in 10 ml phosphate buffers pH (7.4, 6.8), 0.1N HCl (pH 1.6) and water, pre-equilibrated at 37ºC contained in flask. The flask was shaken in horizontal water bath shaker for 48 hours at 200 rpm. The resulting slurry was filtered through 0.45µm membrane filter and absorbance of compounds **7, 8** and Finasteride was determined at their respective wavelengths (λ) 269, 276 and 203 nm using Lambda 35 UV/VIS spectrometer. The concentration of compounds was determined from previously calculated $E^{1\%}_{1cm}$ in different media.

$$\text{Concentration of drug} = \frac{\text{Absorbance}}{E^{1\%}_{1cm}} \times \text{Dilution factor}$$

Enthalpy of Solution

Enthalpy of solution of compound **7, 8** and standard drug Finasteride were determined by Isoperibol solution calorimetry (ISC) in phosphate buffer at pH (pH 7.4, 6.8), 0.1N HCl (pH 1.6) and water at 37°C. Phosphate buffer was kept in reaction vessel i.e. silvered Dewar flask of 25 ml capacity and drug was filled into batch adaptor of volume 0.9 ml, sealed on both sides with '0' rings and cover glass. The batch adaptor holding the drug was inserted into the Dewar flask containing buffer. The combined unit was then lowered to the calorimeter bath. The glass stirrer was rotated at 100 revolutions/min. and was allowed to equilibrate for about 1.5 hr, after which electrical calibration was performed which impart a known heating signal to contents of Dewar flask [57]. The sample cover glass were shattered automatically by means of plunger and heat output was integrated to enthalpy of solution by using following formula.

$\Delta H = Q_{corrected}/n$

ΔH = enthalpy of solution (kJ/mol)

n= number of moles

$Q_{corrected}$ = heat absorbed or released (kJ)

Powder Dissolution Studies

Powder dissolution studies of compound **7, 8** and standard drug Finasteride were performed on dissolution test apparatus (USP-1, basket method) in phosphate buffer (pH 7.4, 6.8), 0.1N HCl (pH 1.6) and water at 37°C for 6 hours. For powder dissolution, 50 mg of sample was filled in gelatin capsule and placed in a basket assembly and basket was rotated at 150 rpm, attached to dissolution apparatus holder, immersed in 900 ml dissolution media. Sample solution 5 ml each of phosphate buffer (pH 7.4, 6.8), 0.1N HCl (pH 1.6) and water was withdrawn with replacement at 5, 10, 15, 30, 45 (minutes), 1, 1.5, 2, 3, 5, 6 (hrs) minutes and filtered through 0.45 µm membrane filter. The same procedure was followed with empty capsule (blank). The concentration of compound **7, 8** and standard drug Finasteride were determined spectrophotometrically by measuring absorbance at their respective wavelength (λ) 269, 276, 203 nm. Powder dissolution rate and release profile were determined by plotting a graph between % release vs. time and compared with that of pure drug [58].

Determination of pKa

pKa of synthesized compounds were determined by UV/VIS spectrometry method. Different buffers of pH 1.6, 4.2, 5.8, 7, 8 and 9.2 were prepared. Stock solution of drug (0.01 mg/mL) was prepared in each buffer. An UV scan of each stock solution was taken and λ_{max} was noted down. Two different wavelengths at a variable pH was selected and absorbance of each solution was determined at selected wavelengths. The ratio of absorbance at selected wavelengths was plotted against the pH. As a result, a sigmoid curve was obtained and the pKa was determined from the inflection point as normal [59].

Octanol-Water Partition Coefficient (Log P)

Partition coefficient of synthesized compounds **7, 8** and standard drug Finasteride was determined by shake flask method. The two phases (water and 1-octanol) were mutually saturated before use by taking them together in 1:1 v/v ratio and shaking them on a thermostatically regulated shaker bath for overnight. Then both the phases were separated with the help of separating funnels. An accurately weighed amount of drug (50 mg) was added to a mixture of 5 mL of pre–saturated organic phase and 5 mL of pre–saturated aqueous phase in 25 mL conical flasks. These conical flasks

were shaken for 24h on a shaker bath at 37 ± 1ºC. The mixture was subsequently centrifuged to separate the aqueous and non–aqueous phases. The contents were filtered through 0.45µm membrane filter and concentration was determined spectrophotometrically by taking absorbance of compounds **7, 8** and Finasteride at their respective wavelengths 269, 276 and 203 nm. The two phases were separately analyzed for the drug content [60]. The partition coefficient of the drugs 'P' was calculated using the formula:

$$\log\ P_{oct/wat} = \log\left(\frac{[solute]^{un-ionized}_{octanol}}{[solute]^{un-ionized}_{water}}\right)$$

2D-QSAR

Computer aided drug designing based on quantitative structure activity relationship (QSAR) is the study of the quantitative relationship between the experimental activity of a set of compounds and their physicochemical properties. Different statistical approaches are used while building a QSAR model, where experimental information associated with biological activity, is used as dependent variable. In the present study, all computational work (2D- QSAR) was performed using Vlife MDS 4.3 QSAR plus software on a HP Pentium IV 2.80 GHz Processor/Microsoft Win XP Home Edition system.

Data set

Twenty six molecules belonging to steroidal lactams, 17-a-Aza, 17-Oximino and 17-Oxo table 1 as 5α-reductase inhibitors, were taken from literature and used for QSAR analysis [48,56]. The above reported series of steroidal 5α-reductase inhibitors showed variance in their structure and potency. Two-dimensional (2D) structures were constructed using Chemdraw Ultra 8.0, and then converted to three-dimensional (3D) structures in same software. All 3D molecules were subjected to energy minimization using molecular mechanics (MMFF) and conformational analysis using Montocarlo conformational search until the root mean square (RMS) gradient value reaches a value smaller than 0.001 kcal/molÅ. Molecules after energy minimization and its physicochemical descriptors were calculated table 2.

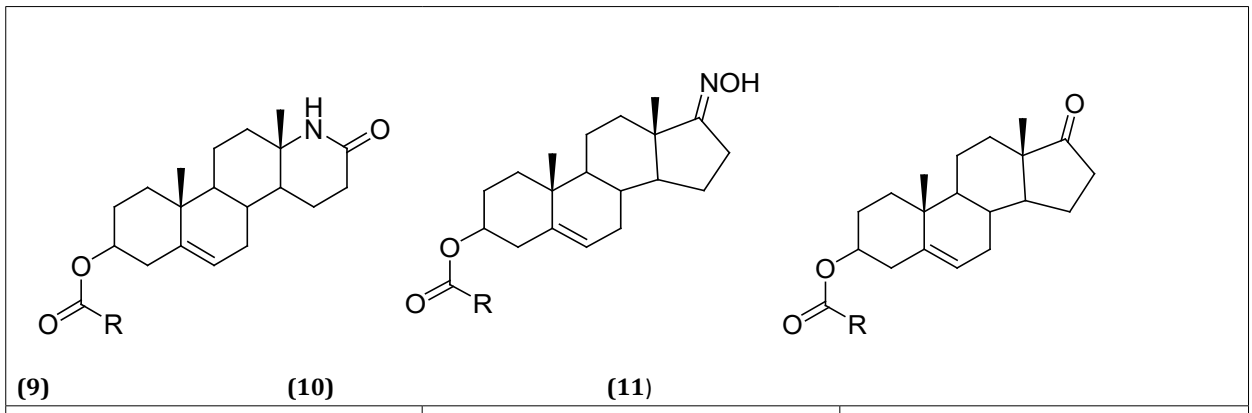

Table 1: Series of 3β-substituted esters of 17 Lactam, 17-Oximino, 17-Oxo androstane steroidal derivatives.

Biological activity

Cytotoxicity-inducing activity data IC50 (μM) of the molecules table 2 were taken from the published reports [48,56]. The experimental IC50 values were evaluated by Mosamann method in a MTT assay [61,62], using prostate cancer cell lines (DU-145) and represents 50% inhibition of this enzyme. Compounds having pIC_{50} ranging from 3.8 to 5.2 has been considered as active. The negative logarithm of the measured IC_{50} (μM) [pIC_{50} = -log (IC_{50})] was used as dependent variable for 2D studies and it is listed in table 2.

Compound No	Actual/ Observed Activity	Predicted Activity
9a	5.148	5.091
9b	4.645	4.638
9c	5.124	5.118
9d	5.08	3.626
9e	4.821	4.923
9f	5.244	5.343
9g	5.148	4.991
9h	5.283	5.023
9i	5.022	5.061
9j	4.48	4.697
10a	5.318	5.133
10b	5.42	5.557
10c	5.512	5.516
10d	5.431	5.497
10e	5.537	5.75
10f	5.267	5.175
10g	5.468	5.608
10h	5.187	5.245
10i	5.22	5.24
10j	5.638	5.638
11a	4.943	4.915
11b	4.906	5.037
11c	5.06	4.997
11d	4.924	4.965
11e	4.95	4.808
11f	4.924	4.83

Table 2: Observed and Predicted activities of compounds.

Molecular Descriptors

Energy-minimized geometry was used for calculation of descriptors, a total of 240 2D descriptors were calculated, eventually reduced to 155 after applying invariable column selection. The steric, topological, electronic, Semi-empirical, thermodynamic, molecular, and structural descriptors calculated were consists of chiV6chain, chiV4pathcluster, IdwAverage (steric), chi1, chi5, chiV0, chiV3, chiV4, chiV5, 3PathCount, chi6chain, chiV6chain, chiV3Cluster, 3ClusterCount, chi4pathCluster, chiV4pathCluster, 4pathClusterCount, kappa3, k1alpha, k2alpha, VChi 3 cluster, VChi 4 cluster, VChi 5 path, Kier shape 2, Kier alpha 1, Kier alpha 3, Kier symmetry index, Chi 0, Chi 2, Chi 3 cluster, Chi 5 path, VChi 1, VChi 3 path, VChi 4 path, VChi 4 path/ cluster, Kier shape 1, Kier shape 3, Kier alpha 2, Kier flexibility, Kier steric descriptor, Delta Chi 0, Delta Chi 2, Delta Chi 3 cluster, Delta Chi 5 path, difference chi 1, Delta Chi 3 path, Delta Chi 4 path, Delta Chi 4 path/cluster, difference chi 0, difference chi 2, charge index 1, charge index 3, charge index 5, charge index 7, charge index 9, valence charge index 2, valence charge index 4, valence charge index 6, valence charge index 8, valence charge index 10, bound charge index 2, k2alpha, Chi 5 path, 0PathCount, (topological), Max. positive charge, max. positive hydrogen charge, local dipole index, relative negative charge, hydrophobic SA–MPEOE, negative charged polar, max negative charge, total positive charge, charge polarization, polarity parameter, relative positive charge, +ve potential surface area, -ve potential surface area, most +ve potential, most -ve potential, average potential, average +ve potential, average -ve potential, most +ve and -ve potential distance, average potential, average +ve potential, average -ve potential (electronic), heat of formation, HOMO energy, LUMO energy, sum of absolute charges, X compDipole, Y compDipole, Z compDipole, dipole moment, quadrupole 1, quadrupole 2, quadrupole 3, QM dipole X, QM dipole Y, QM dipole Z, QM dipole magnitude, XX polarizability, YY polarizability, ZZ polarizability, XY polarizability, XZ polarizability, YZ polarizability, average polarizability, XA most hydrophobic, XA average hydrophobicity, XA most hydrophobic hydrophilic distance, XK hydrophobic area, XK most hydrophobic, XK most hydrophilic, XK average, XK most hydrophobic hydrophilic distance, SA hydrophobic area, SA hydrophilic area, SA most hydrophobic, SA most hydrophilic, SA average, SA average hydrophobicity, SA average hydrophilicity, SA most hydrophobic hydrophilic distance, SK hydrophobic area, SK hydrophilic area, SK most hydrophobic, SK most hydrophilic, SK average, SK average hydrophobicity, SK average hydrophilicity (semi-empirical) [63].

Selection of training and test set

A data set of 26 molecules belonging to esters of 3β-substituted esters of 17a-Aza, 17-Oximino, 17-Oxo androstane derivatives as 5α-reductase inhibitors were taken from the literature and used for QSAR study [49, 61, 62].Different methods such as Genetic Algorithm, Simulated Annealing (SA), Stepwise (Forward and Forward-Backward) were employed to develop models. The dataset can be divided into training set and test set by random (R) and sphere exclusion (SE) method for multiple linear regression (MLR), principal component regression (PCR), partial least squares (PLS) model. Molecules are randomly distributed into the training and test by random selection approach, whereas, in classical sphere exclusion algorithm, each selected molecule generates a hyper-sphere around itself, and any molecule inside the sphere is excluded from the selection in the train set and driven towards the test set. In the present communication, sphere exclusion algorithm with dissimilarity value of 2.82 showed good distribution of data set into training (18 compounds) and test set (8 compounds) respectively. The number of compounds selected and the diversity among them can be determined by adjusting the radius of the sphere (R). Inhibitory activity i.e. pIC_{50} has been considered as dependent variable and the remaining descriptors as independent parameters.

Regression analysis

QSAR is a parametric approach applied to set of series of compounds in order to understand their mechanism of action and important contributory structural factors responsible for activity. In this regard selected physicochemical or structural parameters were used as the correlative parameters and related to the observed biological activity of the 26 molecules by regression analysis MLR, PCR and PLS as statistical approaches. Statistical measures were used for the evaluation of QSAR models were the number of compounds in regression n, multiple correlation coefficient (r), coefficient of determination (r^2), number of descriptors in a model k, F-test (Fisher test value) for statistical significance F, cross-validated correlation coefficient q^2, predictive squared correlation coefficients pred_r^2, coefficient of correlation of predicted data set pred_r^2se and standard error (SE) of estimation r^2se and q^2se. The regression coefficient r^2 is a relative measure of fit by the regression equation. The correlation coefficient values must be closer to 1.0 that represents the better fit of the regression. The F-test reflects the ratio of the variance explained by the model and the variance due to the error in the regression. High values of the F-test indicate that the model is statistically significant. Predictive r^2 (r^2_pred) is the one of the validation parameter, that was calculated for evaluating the predictive capacity of the model and if its value greater than 0.5, means of the QSAR model has good predictive capacity. The number of statistical models were developed using MLR, PCR and PLS based regression methods coupled with forward, forward backward, genetic algorithm and simulated annealing method and correlated the biological activity with the physico-chemical descriptor values. The cross-correlation limit was set at 0.7, number of variables in the final equation obtained were four in all PCR, MLR and PLS and term selection criteria as r^2, F-test 'in,' at 4 and 'out' at 3.99, r^2, and F-test. Variance cut off was set at 0.1, scaling to auto scaling, and number of random iterations to 10 and seed number 910.

MLR is a method used for modelling linear relationship between a dependent variable Y (pEC_{50}) and independent variable X (2D descriptors). MLR is based on least squares: the model is fit such that sum-of-squares of differences of observed and a predicted value is minimized. MLR estimates values of regression coefficients (r^2) by applying least squares curve fitting method. The model creates a relationship in the form of a straight line (linear) that best approximates all the individual data points. In regression analysis, conditional mean of dependant variable (pEC_{50}) Y depends on (descriptors) X. MLR analysis extends this idea to include more than one independent variable.

Regression equation takes the form

$Y = b1 * x1 + b2 * x2 + b3 * x3 + c$

where Y is dependent variable, 'b' s are regression coefficients for corresponding 'x's (independent variable), 'c' is a regression constant or intercept [64,65].

PLS regression method

PLS analysis is a popular regression technique which can be used to relate one or more dependent variable (Y) to several independent (X) variables. PLS relates a matrix Y of dependent variables to a matrix X of molecular structure descriptors. PLS is useful in situations where the number of independent variables exceeds the number of observation, when X data contain collinearities or when N is less than 5 M, where N is number of compound and M is number of dependant variable. PLS creates orthogonal components using existing correlations between independent variables and corresponding outputs while also keeping most of the variance of independent variables. Main aim of PLS regression is to predict the activity (Y) from X and to describe their common structure [66]. PLS is probably the least restrictive of various multivariate extensions of MLR model. PLS is a method for constructing predictive models when factors are many and highly collinear.

PCR method

PCR is a data compression method based on the correlation among dependent and independent variables. PCR provides a method for finding structure in datasets. Its aim is to group correlated variables, replacing the original descriptors by new set called principal components (PCs). These PCs uncorrelated and are built as a simple linear combination of original variables. It rotates the data into a new set of axes such that first few axes reflect most of the variations within the data. First PC (PC1) is defined in the direction of maximum variance of the whole dataset. Second PC (PC2) is the direction that describes the maximum variance in orthogonal subspace to PC1. Subsequent components are taken orthogonal to those previously chosen and describe maximum of remaining variance, by plotting the data on new set of axes, it can spot major underlying structures automatically. Value of each point, when rotated to a given axis, is called the PC value. PCA selects a new set of axes for the data. These are selected in decreasing order of variance within the data. Purpose of principal component. PCR is the estimation of values of a dependent variable on the basis of selected PCs of independent variables [67,68].

Model validation

Model validation is being done to analyse the internal stability and predictive ability of the QSAR models. The best way to evaluate quality of regression model is internal and external validation. Internal validation is carried out using leave one out (q^2, LOO) method. For calculating q^2 each molecule in the training set was eliminated once from training set and the activity of eliminated molecule was predicted by using model developed by the remaining molecules. This q^2 described the internal stability of the model [63] and is expressed as shown in equation (Eq A.1)

$$q^2 = 1 - \Sigma (Y\ pred - Y\ act)\ 2\ / \Sigma (Y\ act - Y\ mean) \quad \text{(Eq A.1)}$$

Secondly, the predictive ability of the model i.e. external validation was confirmed by comparing the observed value of the test set molecules with predictive value of test molecules and is indicated by predicted r^2 as shown in equation (Eq A.2)

$$Pred\_r^2 = 1 - \Sigma (Y\ pred\ (Test) - Y\ Test)\ 2\ / \Sigma (Y\ Test - Y\ Training) \quad \text{(Eq A.2)}$$

In silico Pharmacokinetic Studies

In order to better understand and correlate the synthesized compounds with actual biological activity, various physicochemically significant descriptors and pharmacokinetically relevant properties were predicted using PreADMET version 2.0software. All the analogues were neutralized and minimized before being used by software. The synthesized compounds were evaluated considering Lipnski's rule of 5 and other features which also accounted for their 'druggable' pharmacokinetic profile [69].

Result and Discussion

Synthesis

For the synthesis of the targeted compounds **7-8**, 3β-hydroxy-17a-aza-D-homo-5-androsten-17-one **(6)** was used as starting material. The 3β-hydroxy-17a-aza-D-homo-5-androsten-17-one **(6)** was synthesized from 17-Oxo-5-androsten-3β-yl acetate **(4)** according to the literature (Scheme 1) [70-72]. Representative esters **7** and **8** were prepared by treating 3β-hydroxyl function of 17a-aza-D-homo-5-androsten-17-one with various acids in dichloromethane in the presence of dicyclohexylcarbodiimide (DCC) according to recently published reports from our laboratory as shown in (Scheme 2) [48]. In the esterification reaction, DCC acts as dehydrating agent which forms an O-acylurea called acid– DCC complex, similar to an acid anhydride or acyl halide. This is followed by attack of alcohol on carboxylic carbon of acid–DCC complex, as a nucleophilic catalyst to give esters and dicyclohexyl urea as side product [73].

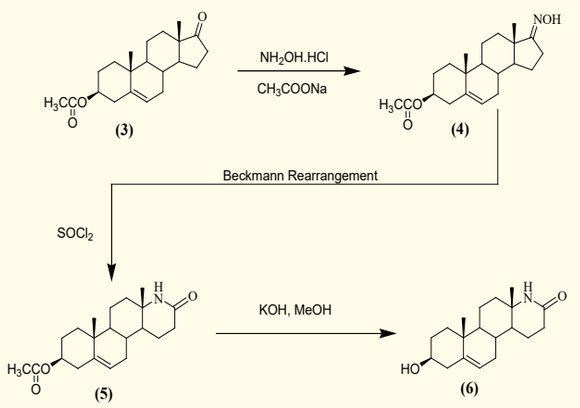

Scheme 1

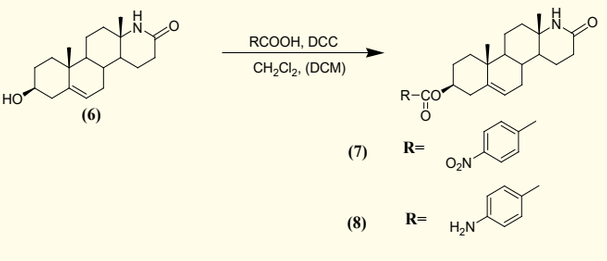

Scheme 2

Characterization

Differential Scanning Calorimetry (DSC) provides the information of crystallization, solid state transition, desolvation, melting, decomposition and purity of sample. Thermodynamic relation between different phases, enantiotropic and monotropic transitions, and the stability relationship among various crystalline forms can also be studied using DSC. Figure 3-5 and table 3 represents the DSC scan and the interpretation of thermal characteristics of the compound 7, 8 and Finasteride respectively. Single sharp endothermic peaks indicating the extremely pure and crystalline nature of the synthesized compounds 7 and 8 were observed at 206.33ºC (ΔH_f248.1 J/g), 188.77°C (ΔH_f25.82 J/g) respectively, whereas sharp endothermic peak at 258.40ºC (ΔH_f20.68 J/g) was observed for finasteride. Further, absence of transition endotherm in these DSC scan suggested that reactant has been completely converted in to desired products with no intermediate, thus free from impurity.

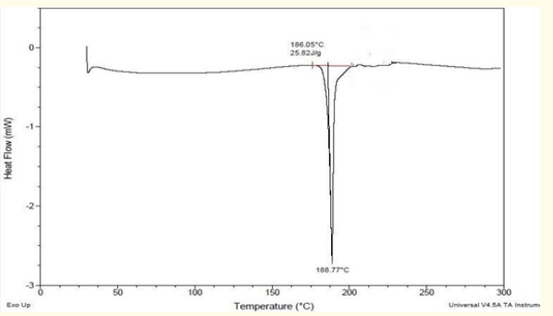

Figure 3: DSC scans of 17-Oxo-17a-aza-D-homo-5-androsten-3β-yl 4-nitrobenzoate (7).

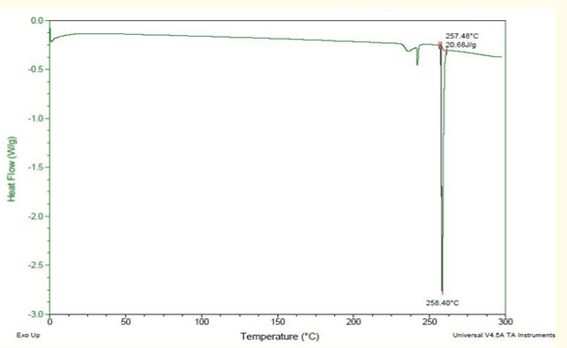

Figure 4: DSC scans of 17-Oxo-17a-aza-D-homo-5-androsten-3β-yl 4-aminobenzoate (8).

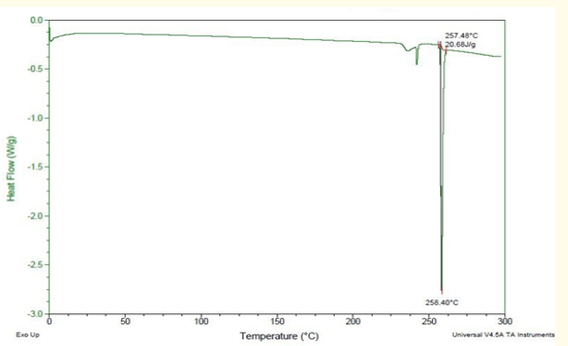

Figure 5: DSC scans of Finasteride (F).

Compounds	Melting endotherm (°C)	Enthalpy of fusion (J/g)
7	206.33	248.1
8	188.77	25.82
Finasteride	258.40	20.68

Table 3: Thermal characteristics of compound 7, 8 and Finasteride interpreted by differential scanning calorimetry.

X-ray powder diffraction patterns confirming the crystalline nature of both compounds 7 and 8 are shown in figure 6 and 7. However the appearance of more characteristics and diffraction peaks in PXRD data of compound 8, suggest its more crystalline nature as compared to compound 7. The characteristic peaks at 10.95°, 7.25°, 18.49°, 21.97° (100% relative intensity), 28.38° has been observed in PXRD pattern of compound 7, whereas compound 8 has shown characteristic peaks at 8.49°, 10.19°, 11.49°, 11.63º, 12.23º, 16.00º, 18.14º, 18.66º, 18.98º (100% relative intensity), 20.24°. Position of 2θ value along the peak intensity are given in table 4 and table 5 respectively.

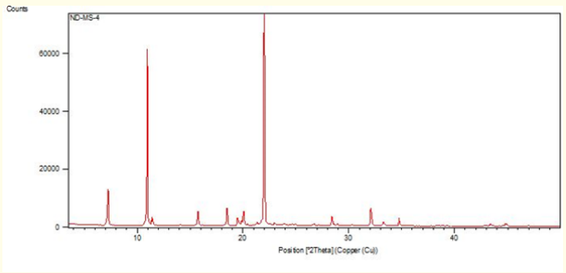

Figure 6: PXRD of 17-Oxo-17a-aza-D-homo-5-androsten-3β-yl 4-nitrobenzoate (7).

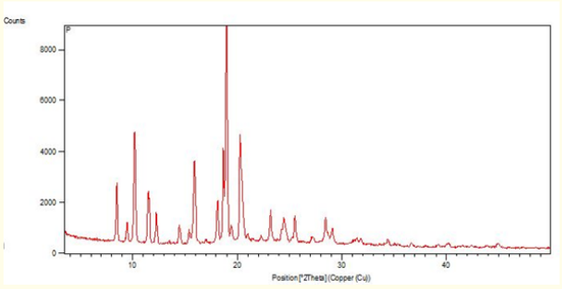

Figure 7: PXRD of 17-Oxo-17a-aza-D-homo-5-androsten-3β-yl 4-aminobenzoate.

Pos. [°2Th.]	FWHM [°2Th.]	d-spacing [Å]	Rel. Int. [%]	Area [cts*°2Th.]
7.2526	0.0836	12.17897	17.63	1014.84
9.8951	0.0836	8.93162	0.17	9.87
10.9664	0.0836	8.06142	87.63	5045.51
11.3268	0.0335	7.80573	2.6	59.76
11.426	0.0502	7.73819	4.12	142.28
14.0781	0.1338	6.2858	0.5	46.03
14.6058	0.1338	6.05986	0.17	15.51
15.757	0.1171	5.61964	6.84	551.37
16.1775	0.0836	5.47451	0.3	17.44
18.4903	0.0836	4.79463	8.64	497.33
19.4699	0.0836	4.55555	3.94	226.81
19.8543	0.0669	4.4682	2.4	110.74
20.0496	0.1004	4.42512	7.05	486.74
20.3881	0.1004	4.35241	0.72	49.87
21.3362	0.0502	4.16108	1.91	65.92
21.6982	0.0836	4.09249	2.82	162.37
21.9755	0.1171	4.04146	100	8060.39
22.9453	0.0669	3.87279	1.63	74.99
23.9405	0.1004	3.714	0.65	45
24.3933	0.1338	3.64608	0.46	42.67
24.6242	0.1171	3.61241	0.7	56.79
24.8813	0.0669	3.57566	0.73	33.78
26.6632	0.1338	3.34061	0.99	91.64
27.1223	0.1004	3.28509	0.37	25.89
28.3842	0.0816	3.14186	4.65	353.33
28.9378	0.0816	3.08299	1.01	76.59
30.2753	0.0816	2.94977	0.5	38.3
31.2576	0.1632	2.85927	0.33	49.5
32.053	0.102	2.79011	7.99	758.7
33.2723	0.0816	2.6906	2.03	154.21
34.7385	0.0408	2.58032	3.92	148.88
35.9768	0.0408	2.4943	0.31	11.86
37.724	0.3264	2.38269	0.05	15.82
38.3162	0.1632	2.34721	0.26	39.57
38.7809	0.0816	2.32015	0.16	11.79
39.353	0.204	2.28773	0.11	20.56
41.265	0.2448	2.18604	0.06	13.36
42.8839	0.2448	2.10719	0.18	40.78
43.3681	0.0612	2.08477	1.03	58.49
44.529	0.0816	2.03308	0.23	17.42
44.771	0.0612	2.02265	1.05	59.72
44.8724	0.0612	2.01832	1.24	70.84
46.9112	0.0612	1.93524	0.25	14.26
47.5433	0.4896	1.91097	0.07	31.92
49.1599	0.1224	1.85185	0.12	13.59

Table 4: Position of 2θ value along the peak intensity of compound 7.

Pos. [°2Th.]	FWHM [°2Th.]	d-spacing [Å]	Rel. Int. [%]	Area [cts*°2Th.]
8.4925	0.1338	10.41203	26.95	305.21
9.4688	0.1171	9.34049	8.5	84.2
10.1981	0.1673	8.67409	50.87	720.18
11.4945	0.1338	7.69856	23.54	266.6
11.6323	0.0502	7.6077	18.94	80.43
12.2374	0.0669	7.23284	14.26	80.74
13.4879	0.1338	6.56494	1.35	15.33
14.449	0.0836	6.13037	8.29	58.66
15.3985	0.0836	5.75441	6.49	45.9
16.0065	0.2007	5.53719	26.62	452.15
16.9895	0.1338	5.21895	1.88	21.27
18.0581	0.0669	4.91246	15.61	88.42
18.1492	0.1004	4.888	19.79	168.06
18.6675	0.1004	4.75345	43.49	369.39
18.9803	0.1506	4.67579	100	1274.07
19.4403	0.1338	4.5662	8.92	101.04
20.247	0.1171	4.38604	46.99	465.65
20.9874	0.1004	4.23295	4.83	40.99
22.2891	0.1338	3.9886	4.12	46.7
23.2229	0.1506	3.83029	15.7	200.02
24.453	0.1171	3.64032	12.6	124.82

25.4616	0.1673	3.49836	11.77	166.68
27.2586	0.2342	3.27168	3.77	74.65
28.4872	0.1338	3.13331	12.85	145.55
29.1289	0.1673	3.06573	7.27	102.9
31.427	0.1004	2.8466	3.34	28.36
31.8551	0.1673	2.80932	3.5	49.48
34.3913	0.2342	2.60773	3.13	62.05
35.0775	0.1004	2.55827	1.48	12.56
36.679	0.2007	2.45017	1.63	27.76
37.9873	0.2676	2.36874	0.49	11.19
39.2601	0.2342	2.29483	1.12	22.14
40.2002	0.1673	2.2433	1.94	27.46
41.3652	0.5353	2.18278	0.53	24.15
42.5446	0.4015	2.12496	0.49	16.79
43.8685	0.4015	2.06385	0.71	24.26
45.01	0.2342	2.01413	1.77	35.04
47.3147	0.2448	1.91967	0.62	17.3

Table 5: Position of 2θ value along the peak intensity of compound 8.

Crystal structures of novel azasteroids **7** and **8** were further determined using material studio and respective crystallographic parameters are shown in table 6 and table 7. Compound 7 crystallizes in triclinic crystal system with space group P1 as shown in figure 8 (b), whereas compound 8 crystallizes in monoclinic crystal system with space group P2 as shown in figure 9 (b).

Cell	Triclinic
Space group	*P-1*
Cell lengths	a = 8.6316; b =6.2369; c = 4.9074
Cell angles	α = 81.2891; β = 100.9912; ϒ = 108.7708
Cell volumes	244.391

Table 6: Crystallographic data of compound 7.

Cell	Monoclinic
Space group	P-2
Cell lengths	a = 11.6161 ; b = 22.8817; c = 10.6548
Cell angles	α = 90.0; β = 116.1263; ϒ = 90.0
Cell volumes	2542.65

Table 7: Crystallographic data of compound 8.

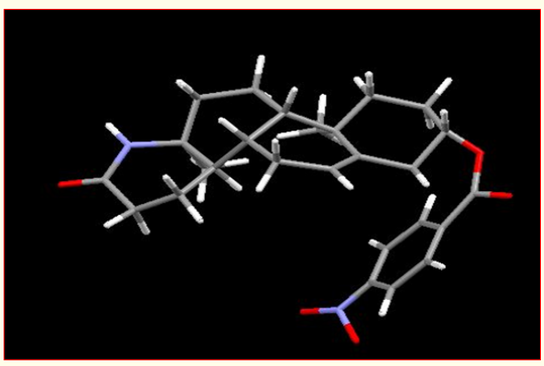

Figure 8a: 17-Oxo-17a-aza-D-homo-5-androsten-3β-yl 4-nitrobenzoate (7).

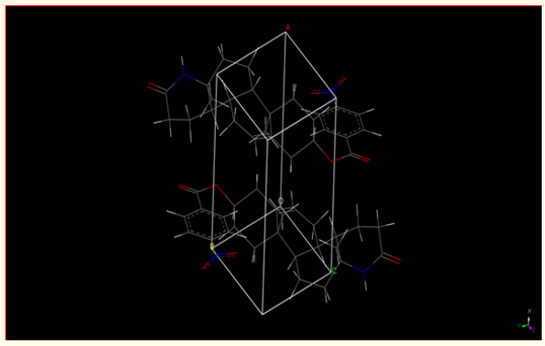

Figure 8b: Arrangement of molecules in unit cell of 17-Oxo-17a-aza-D-homo-5-androsten-3β- yl 4-nitrobenzoate (7).

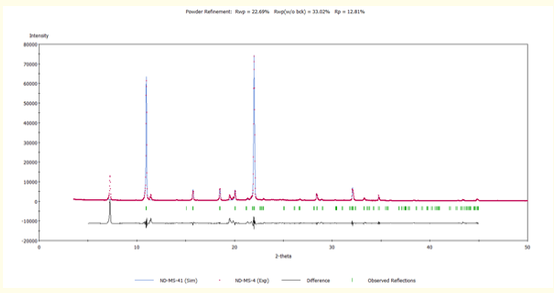

Figure 8c: X-ray intensity as a function of 2θ. Observed (experimental) pattern, calculated (best riveted fit profile) pattern, reflection positions and the difference curve between observed and calculated profile of 17-Oxo-17a-aza-D-homo-5-androsten-3β-yl 4-nitrobenzoate (7).

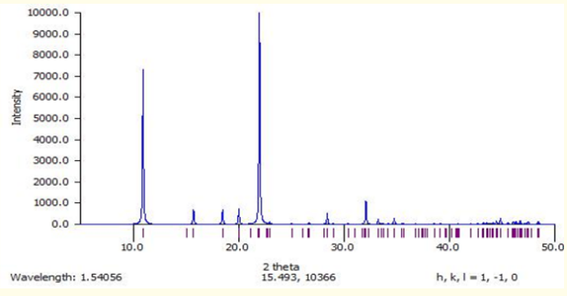

Figure 8d: Simulated PXRD of compound 7.

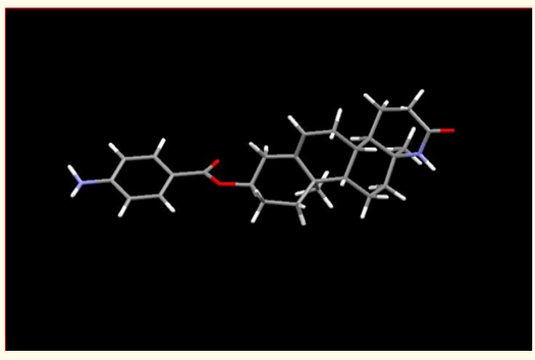

Figure 9a: 17-Oxo-17a-aza-D-homo-5-androsten-3β-yl 4-aminobenzoate (8).

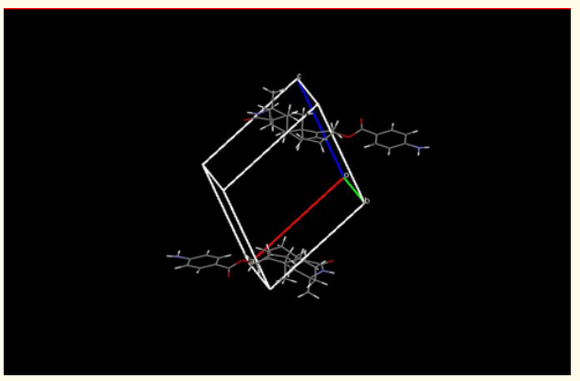

Figure 9b: Arrangement of molecules in unit cell of 17-Oxo-17a-aza-D-homo-5-androsten-3β- yl 4-aminobenzoate (8).

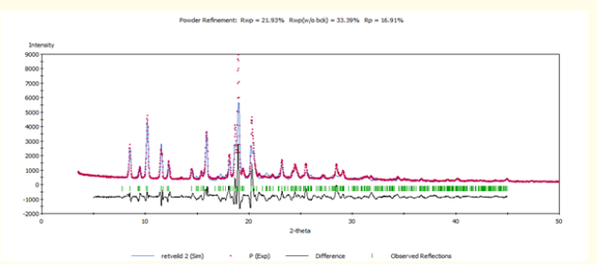

Figure 9c: X-ray intensity as a function of 2θ. Observed (experimental) pattern, calculated (best rietveld fit profile) pattern, reflection positions and the difference curve between observed and calculated profile of 17-Oxo-17a-aza-D-homo-5-androsten-3β-yl 4-aminobenzoate (8).

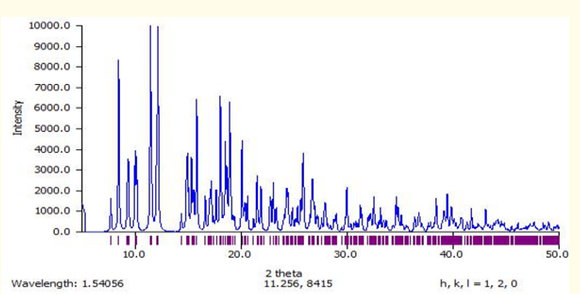

Figure 9d: Simulated PXRD of compound 8.

Physicochemical properties

Solubility of synthesized compounds **7, 8** and reference drug Finasteride were determined in phosphate buffer pH 7.4, 6.8, 0.1N HCl (pH-1.6) and water at 37 C and the results are expressed in mg/mL as shown in table 8. Common pattern for the solubility order i.e. **7** > Finasteride > **8**, has been observed in all the different media, but the maximum solution has been observed in water and 0.1 N HCl for compound **7** and **8** respectively as shown in figure 10. Unique behaviour i.e. high solubility of **7** can be correlated with its less or poor packing energy involved in its less crystalline nature. Such molecules on coming in contact with solvent media have been found to triggers solubilization by disrupting crystal packing. Earlier published report [49] from our laboratories has also indicated the high anti-androgenic activity of **7** within the synthesized series and the maximum activity could be owed to its higher solubility resulting in its better bioavailability.

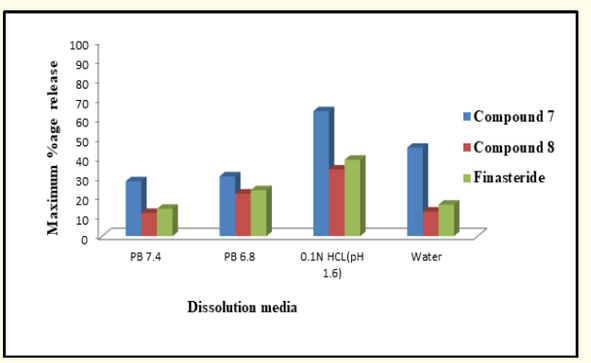

Figure 10: Bar graph representation of solubility (mg/mL) of compound 7, 8 and Finasteride in different solubility media.

Buffers/ Solubility Media	Solubility (mg/mL) ± SD (n = 3)		
	Compound 7	Compound 8	Finasteride
Phosphate Buffer 7.4	0.547 ± 0.01	0.106 ± 0.01	0.164 ± 0.01
Phosphate Buffer 6.8	0.363 ± 0.01	0.090 ± 0.01	0.116 ± 0.02
0.1N HCl (pH-1.6)	0.986 ± 0.04	0.283 ± 0.02	0.292 ± 0.01
Water	1.178 ± 0.02	0.065 ± 0.02	0.111 ± 0.03

Table 8: Solubility (mg/mL) ± SD of compound 7, 8 and Finasteride in different Phosphate buffers (7.4, 6.8), 0.1N HCl (pH-1.6) and water at 37°C.

Calorimetrically determined enthalpy of solution has great potential in characterization of different synthesized compounds. It depends upon the lattice energy, crystal structure and is different for different compounds. Compound **7** and **8** showed endothermic behaviour in phosphate buffer (pH 7.4 and 6.8), 0.1N HCl (pH 1.6) and water shown in table 9 and the absolute value of molar enthalpy of solution followed the order: compound **7** < Finasteride < compound **8**. The higher value of ΔH_{sol} associated with compound 8 indicated its more crystalline nature as compared to compound **7** and results are in agreement with the observation found in PXRD data and their solubility studies.

Buffers/Media	$Q_{corrected}$ (kJ)			Enthalpy of solution (ΔH_{sol}) (kJ/mol) at 37°C		
	Compound 7	Compound 8	Finasteride	Compound 7 n = 0.00663	Compound 8 n = 0.00710	Finasteride n = 0.00806
Phosphate Buffer 7.4	0.20504	0.40284	0.26501	30.92	56.66	32.87
Phosphate Buffer 6.8	0.18629	0.58461	0.27203	28.09	82.23	33.75
0.1N HCl (pH-1.6)	0.03802	0.09743	0.07315	5.73	13.70	9.07
Water	0.07642	0.27959	0.09310	11.52	39.32	11.5

Table 9: Enthalpy of solution (ΔH_{sol}) (KJ/mol) compound 7, 8 and Finasteride in phosphate buffer (7.4, 6.8), 0.1N HCl and water.

The powder dissolution experiment was carried out for 6 hours at 37 ± 0.5ºC using phosphate buffer (pH 7.4, 6.8), 0.1N HCl (pH 1.6) and water as dissolution medium. Comparative percent release rate in all dissolution media are in concordance with solubility studies and follow the order: **7** > finasteride > **8**. The maximum percent release of 60.13%, 32.64% and 36.14% has been observed for the compound **7, 8** and Finasteride in dissolution medium of 0.1N HCl (pH-1.6) at period of 3, 5 and 6 hrs respectively. These observations are in agreement with the solubility profile of the compounds in acidic medium as shown in table 9 and figure 11 (a-d). Interestingly, maximum release of compound **7** was found to be 60.13% drug release in 3hrs, showing better onset release comparing to other compound. Better release profile of compound **7** may be further correlated with its potent anti-androgenic activity and thus considered to be suitable for oral drug delivery system shown in figure 12.

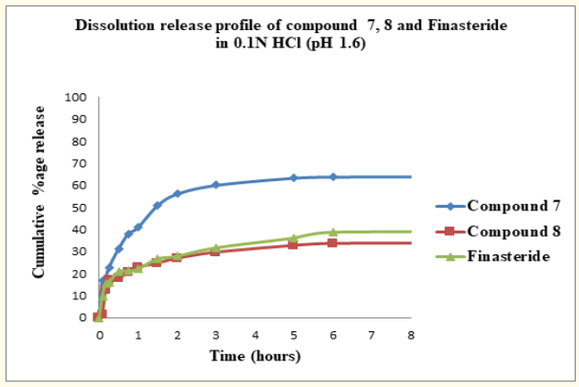

Figure 11c: Comparative percent release profile of Compound **7, 8** and Finasteride in 0.1N HCl (pH 1.6).

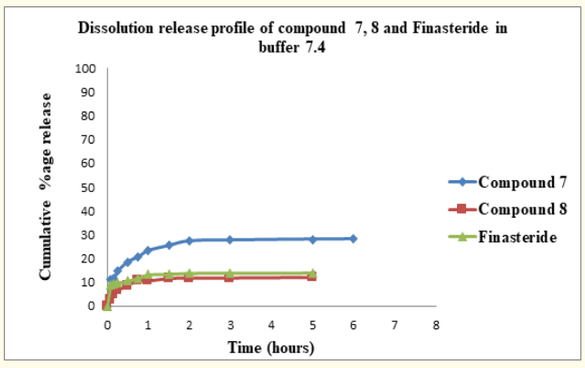

Figure 11a: Comparative percent release profile of compound **7, 8** and Finasteride in phosphate buffer pH 7.4.

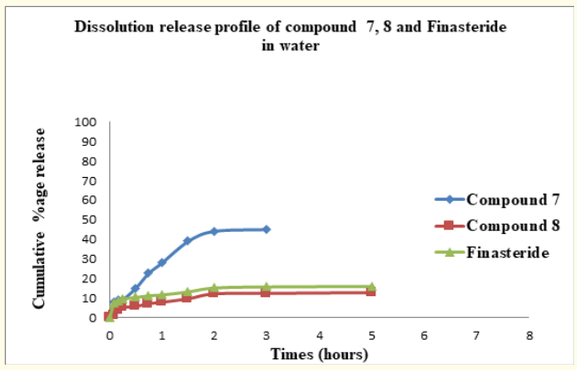

Figure 11d: Comparative percent release profile of compound 7,8 and Finasteride in water.

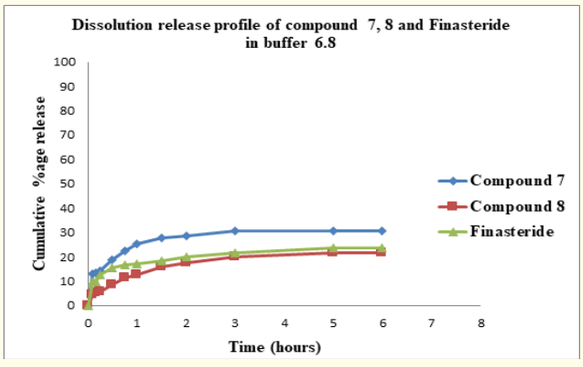

Figure 11b: Comparative percent release profile of compound **7, 8** and Finasteride in phosphate buffer pH 6.8.

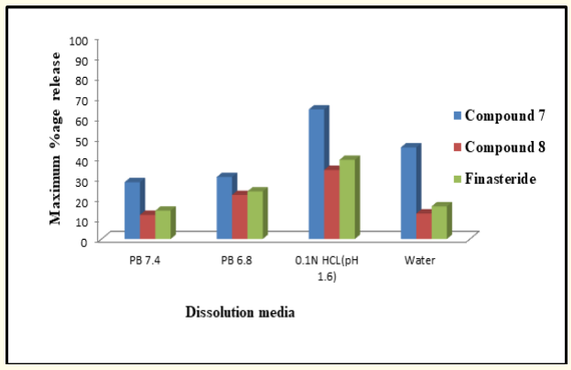

Figure 12: Bar graph representation of maximum percent release of compound 7, 8 and Finasteride in different dissolution media.

An acid dissociation constant, pKa, is a quantitative measure of the strength of an acid in solution. As the majority of drugs are weak acids and/or bases, knowledge of the dissociation constant helps in understanding their different ionic form of molecules, which will be able to diffuse across the membrane with wide range of physiological systems. Weakly acidic nature of the newly synthesised compound **7** and finasteride has been indicated with their value of pka 5.23.and 6.63 respectively. Further appearance of two sigmoid peaks at 7.57 and 5.56, in 17-Oxo-17a-aza-D-homo-5-androsten-3β-yl 4-aminobenzoate **(8)** indicates the presence of two replaceable hydrogens value and its weakly acidic nature. Drug penetration may be attributed mostly to the un-ionized form, thus weak acidic drugs are found to be absorbed better in the acidic medium of stomach, because of their poor dissociation. Weak acidic drugs with poor dissociation are found to be better absorbed in the acidic environment of stomach. Readily diffusion across the cell membrane, thus high bioavailability can be attributed to the lipid soluble un-ionized form of such drugs. Present calculated pka values of the compounds **7** and **8** indicating their better absorption in highly acidic environment of upper GIT shown in figure 13-16.

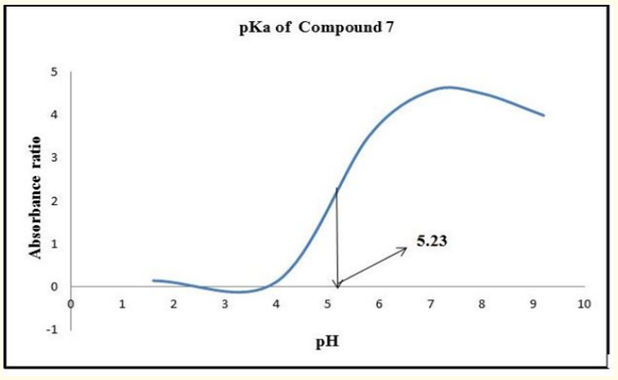

Figure 13: pKa of 17-Oxo-17a-aza-D-homo-5-androsten-3β-yl 4-nitrobenzoate (7).

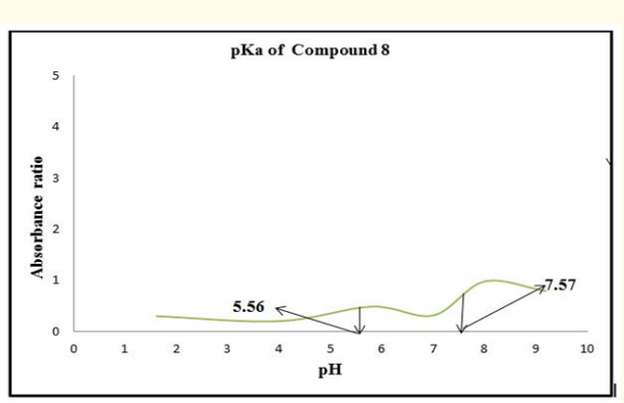

Figure 14: pKa of 17-Oxo-17a-aza-D-homo-5-androsten-3β-yl 4-aminobenzoate (8).

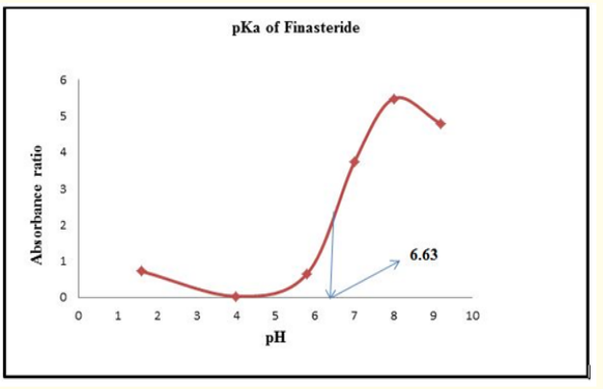

Figure 15: pKa of Finasteride.

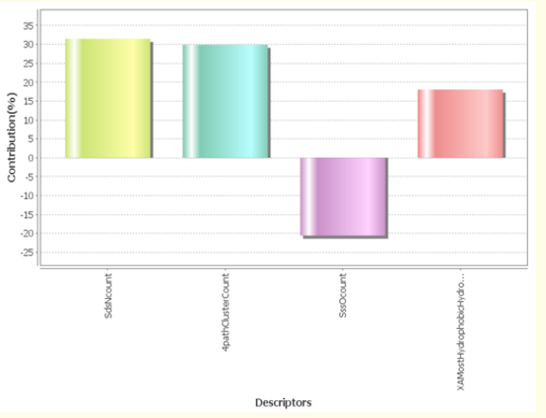

Figure 16: Contribution plot of various descriptors in PLS.

Log P is an estimate of a compound's overall lipophilicity, a value that influence its behaviour in a range of biological processes relevant to a drug discovery, such as solubility, permeability through biological membranes, extent of absorption, hepatic clearance, lack of selectivity and non-specific toxicity. Drugs with low value of log P has been found to have increased ease of formulation and bioavailability, reduced toxicity and non-specific binding. The experimentally obtained Log P of compound **7, 8** and Finasteride in octanol–water system was found to be 3.59 ± 0.095, 3.11 ± 0.056 and 3.18 ± 0.045 respectively shown in table 10. Lipinski's rule states that, in an orally active drug log P should not be greater than 5 and present value of log P for the synthesized compounds, further confirmed their hydrophilic nature with the preference towards aqueous compartments such as blood serum. *In silico*, octanol–water partition coefficient was calculated using Chem draw ultra (12.0) software was found to be 4.92 **(7)**, 3.27 **(8)** and 3.15 (finasteride) in consonance with experimental values.

Compound	LOG P ± SD (n=3)	
	Experimental Value	Predicted Value
7	3.59 ± 0.095	4.92
8	3.11 ± 0.056	3.27
Finasteride	3.18 ± 0.045	3.15

Table 10: Log P ± SD of compound 7, 8 and Finasteride.

Quantitative Structure and Relationship

2D QSAR

With regard to QSAR models, our main aim was to establish a predictive model with reasonable number of logical descriptors to get good generalization performance, which would be further utilized to predict the activity of present compounds or for the synthesis of steroidal molecules with potential to inhibit 5α-reductase enzyme. Selected molecular parameters computed for all the 26 molecules (Table 1) were used to develop QSAR equation by relating their corresponding inhibitory activities i.e. IC_{50} values.

Genetic Algorithms (GA), Simulated Annealing (SA), Stepwise (forward, forward-backward) techniques were used to develop best fit model and model with minimum number of descriptors has considered or found to be the best model. When this point is achieved, no further considerable improvement in the regression coefficient (r^2 and q^2) values were observed even if a new descriptor is added. In the present study MLR, PCR and PLS, methods employing three, four or more variable combinations for combined dataset generated around 400 equations out of which, the reasonable acceptable ones were selected for discussion. The different models generated for better correlation by statistical analysis and their different contribution descriptors are given in table 11.

Models	GA			SA			SW (Forward)			SW (Forward-backward)		
	PCR	MLR	PLS	PCR	PLS	MLR	MLR	PCR	PLS	MLR	PCR	PLS
Equation	Eq A.1	Eq A.2	Eq A.3	Eq B.1	Eq B.2	Eq B.3	Eq C.1	Eq C.2	Eq C.3	Eq D.1	Eq D.2	Eq D.3
N	18	18	18	18	18	18	18	18	18	18	18	18
r^2	0.302	0.446	0.445	0.785	0.807	0.832	0.806	0.790	0.833	0.806	0.790	0.833
q^2	-0.214	0.191	0.217	0.563	0.614	0.630	0.662	0.635	0.671	0.662	0.635	0.671
F value	17.75	3.76	6.061	17.39	31.54	16.09	13.50	17.75	37.49	13.50	17.75	37.49
pred_r^2	-0.287	0.339	0.364	0.819	0.614	0.727	-0.868	0.813	0.736	-0.868	0.813	0.736

Table 11: The different models generated for better correlation by statistical analysis.

Interpretation

Genetic algorithms (GA)

Genetic algorithms are derived from an analogy with the spread of mutations in a population. In this analogy, "individuals" are represented as a one-dimensional string of bits. An initial population of individuals is created, usually with random initial bits. A fitness function is used to estimate the "quality" of an individual, so that the "best" individuals receive the best fitness scores. Individuals with the best scores are more likely to propagate their genetic material to offspring through crossover, in which pieces of genetic material are taken from each parent and recombined to create the child. After many such mating steps, the average fitness of the individuals in the population increases, as good combinations of genes are discovered and spread through the population. Genetic algorithms are especially good at searching problem spaces having a large number of dimensions, since they conduct a very efficient, directed sampling of the large space of possibilities [74-76].

The PCR (Eq B.1), MLR (Eq B.2), PLS (Eq B.3) models predicted the training data having r^2 0.302, 0.446, 0.445 together with q^2 estimating to -0.214, 0.191 and 0.217 respectively.

Model 1

pIC_{50} = 0.7765 (XKAverageHydrophobicity) + 0.3120 (SsNH_2count) + 0.4652 (IdwAverage) +0.3807 (EqB.1)

Model 2

pIC_{50} = 0.2025 (XlogP)+0.0626 (SsNH_2count)+0.0181 (XAHydrophilicArea)+3.0325 (EqB.2)

Model 3

pIC_{50} = 0.2030 (XlogP) + 0.0194 (XAHydrophilicArea) +2.9659 (Eq B.3)

Models with negative/low pred r^2 and q^2 were not found to be significantly satisfactory. Further, simulated annealing of 5 alpha reductase inhibitors was performed to get improved QSAR model. Various descriptors obtained by various methods (MLR, PCR, PLS) under GA; their contributions and significance shown in table 12.

GA			
Descriptor	Category	Contribution	Meaning
XlogP	Physico-chemical	+	Signifies ratio of solute concentration in octanol and water.
SsNH_2count	Topological	+	Total number of –NH_2 group connected with one single bond.
XAHydrophilicArea	Semi-empirical	+	Showing hydrophilic surface area.
XlogP	Physico-chemical	+	Signifies ratio of solute concentration in octanol & water.
XAHydrophilicArea	Semi-empirical	+	Showing hydrophilic surface area.
XKAverage Hydrophobicity	Semi-empirical	+	Average hydrophobic value on the vdW surface
SsNH_2count	Topological	+	Total number of –NH_2 group connected with one single bond.
IdwAverage	Steric	+	Information-based descriptors.

Table 12: Various descriptors obtained by various methods (MLR, PCR, PLS) under GA; their contributions and significance.

Simulated annealing (SA)

Simulated annealing is a global, multivariate optimization technique based on the Metropolis Monte-Carlo search algorithm. The method starts from an initial random state, and wall through the state space associated with the problem of interest by a series of small, stochastic steps. In the problem at hand, a state represents a particular subset of M features, and a step is the replacement of one of these M features with another randomly chosen feature that is not currently in the model. The training error of the resulting model represents the energy or 'fitness' of that state. While downhill transitions are always accepted, uphill transitions are accepted with a probability that is inversely proportional to the energy difference between the two states. This probability is computed using Metropolis' acceptance criterion, p ¼ e) DE/KT, where K is a constant used for scaling purposes, and T is an artificial temperature factor that controls the ability of the system to overcome energy barriers. The temperature is systematically adjusted during the course of the simulation in a manner that gradually reduces the probability of high-energy transitions (in this case, using a Gaussian cooling schedule with a half width of 5 deviation units). To circumvent the problem of selecting an appropriate value for K and ensure that the transition probability is properly controlled, we use an adaptive approach in which K is not a true constant, but rather it is continuously adjusted during the course of the simulation based on a running estimate of the mean transition energy. In particular, at the end of each transition, the mean transition energy is updated, and the value of K is adjusted so that the acceptance probability for a mean uphill transition at the final temperature is some predefined small number (here 0.1%) [76,77].

Model 4

pIC_{50} = 0.3664 (SsOHcount) - 0.0724 (ZcompDipole) + 0.0342 (AlphaR) - 0.1369 (SssOcount) + 4.6720 (Eq C.1)

The generated PCR model Eq C.1 showed high squared r^2 0.788 and pred r^2 0.819, but low F value 17.39 was not found to be significant. PLS regression analysis led to the deviation to another model Eq C.2, with high F value 31.549, but low pred r^2 0.614 value indicated poor correlation between descriptors (SAHydrophobicArea, kappa1, SsOHE-index, SssOE-index) and 5 alpha reductase inhibitor activity.

Model 5

pIC_{50} = 0.0033 (SAHydrophobicArea) + 0.0347 (kappa1) + 0.0413 (SsOHE-index) - 0.0503 (SssOE-index) + 3.0198 (Eq C.2)

The model obtained Eq C.3 by MLR analysis is given below with good statistical parameters r^2 and q^2 0.832, 0.630 respectively. However, the model was rejected on the basis of its low F value 16.090 i.e. variance due to error in regression.

Model 6

pIC_{50} = 0.0070 (vdWSurfaceArea) - 0.0833 (SssOEindex) + 0.0507 (SAMostHydrophobicHydrophilicDistance) + 0.1342 (SdsNE-index) + 1.675 (Eq B.3)

Various descriptors obtained by various methods (MLR, PCR, PLS) under SA; their contributions and significance shown in table 13.

SA			
Descriptor	**Category**	**Contribution**	**Meaning**
vdWSurfaceArea	Steric	+	Total van der Waals surface area of the molecule
SssOE-index	Electrotopological	-	Number of oxygen atom connected with two single bonds.
SAMostHydrophobic HydrophilicDistance	Semi-empirical	+	Distance between most hydrophobic and hydrophilic point on the vdW surface.
SdsNE-index	Topological	+	Number of N atom connected with two double and one single bond
SAHydrophobicArea	Semi-empirical	+	Hydrophobic point on the vdW surface.
kappa1	Steric	+	Signifies first kappa shape index kappa shape index related to steric nature of molecule
SsOHE-index	Electrotopological	+	Number of –OH group connected with one single bond.
SssOE-index	Electrotopological	_	Number of Oxygen atom connected with two single bond.
SsOHcount	Topological	+	Total number of –OH group connected with one single bond.
ZcompDipole	Semi-empirical	-	z component of the dipole moment
AlphaR	Hydrophobic	+	All non-hydrogen atoms in a reference alkane.
SssOcount	Topological	-	Total number of oxygen connected with two single-bonds.

Table 13: Various descriptors obtained by various methods (MLR, PCR, PLS) under SA; their contributions and significance.

Stepwise variable selection

This is the simplest and most commonly used greedy feature selection algorithm in data mining and QSAR. Given a set of N input features, the method starts by evaluating all possible models containing a single feature, and selecting the one with the lowest training error. Then, all possible two-feature models consisting of the feature selected in the previous step and one other feature from the remaining N 1 input features are evaluated, and the one

with the lowest training error is added to the set. This process continues until the training error no longer improves or until the desired number of features is selected [78].

The models (7-12) were developed using Stepwise forward and Stepwise forward-backward (SW-F, SW-FB) methods, with cross correlation limit set to 0.5 and selected criteria as q^2. Multiple linear regression with SW-F (Model 7) and SW-FB (Model 10) methods predicted the training data with same r^2 of 0.806 as shown in Eq D.1. Further, suitable satisfying statistical parameters of r^2 0.79 were worked out with PCR using SW-F (Model 8), SW-FB (Model 11) respectively as shown in Eq D.2. Predictive ability of generated QSAR models were evolved by q^2 employing LOO method, (0.662, 0.662) and (0.635, 0.635) respectively. However, model with poor or negative pred r^2 -0.860 and low F value 13.50 (MLR) were rejected.

Model 7 (SW-F: MLR) and Model 10 (SW-FB: MLR)

pIC_{50} = 0.0486 (SsOHE-index) - 0.1124 (ZcompDipole) - 0.0213 (XAHydrophilicArea) + 0.0274 (XKMostHydrophobic HydrophilicDistance) + 5.8746 (Eq D.1)

Model 8 (PCR) and Model 11(PCR)

pIC_{50} = 0.0394 (SsOHE-index) - 0.0594 (ZcompDipole) + 0.0961 (chi4pathCluster) - 0.1228 (SssOcount) + 4.7733 (Eq D.2)

The best 2D QSAR model for the prediction of inhibitory activity was obtained by applying PLS of SW-F (Model 9) or SW-FB (Model 12). Both these models have excellent but same statistical parameters of r^2 0.833, q^2 0.671, F value 37.498, and pred r^2 0.736 as shown in Eq D.3. Greater value > 0.5 for q^2 LOO imply that models has good predictive ability.

Model 9 (PLS) and Model 12(PLS)

pIC_{50} = 0.0367 (SsOHE-index) - 0.0575 (ZcompDipole) - 0.2139 (SssOcount) + 0.0027 (SAHydrophobicArea) + 4.0688 (Eq D.3)

The 2D model obtained showed that topological interactions and semi empirical plays important role in the determination of 5 alpha reductase inhibitory activity. SsOHE-index and SssOcount in Eq C.3, are topological descriptors; whereas ZcompDipole and SAHydrophobicArea are semi empirical descriptors. SsOHE-index; a Electrotopological descriptor, represents the indices for number of –OH group connected with one single bond. It is positively correlated with biological activity that means higher is the SsOHE-index; higher will be the inhibitory activity against human 5α-reductase. SssOcount is an another electrotopological descriptor but somewhat with lower and negative contribution towards inhibitory activity, and it defines the total number of oxygen connected with two single bonds. ZcompDipole signifies the z component of the dipole moment (external coordinates) and its negative correlation suggests that higher is the ZcompDipole, the lower will be inhibitory activity against human 5α-reductase. SA Hydrophobic Area is a hydrophobic surface area descriptor also contributes positively, means more is the SAHydrophobicArea, more will be the 5α-reductase inhibitory activity. The fitness plot of observed, predicted activities of the 26 molecules has been given in figure 17-19 and various descriptors obtained by various methods (MLR, PCR, PLS) under SW-F, SW-FB; their contributions and significance shown in table 14 and table 15.

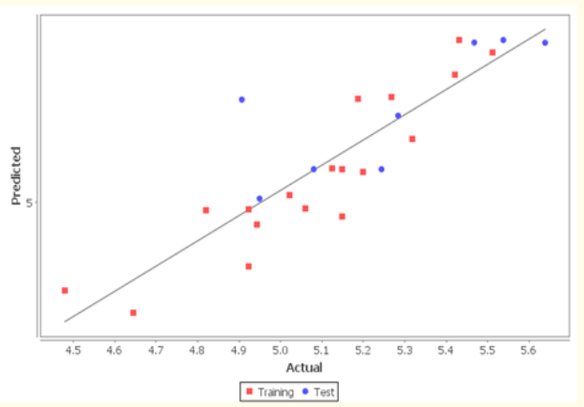

Figure 17: Fitness plot of PLS Model.

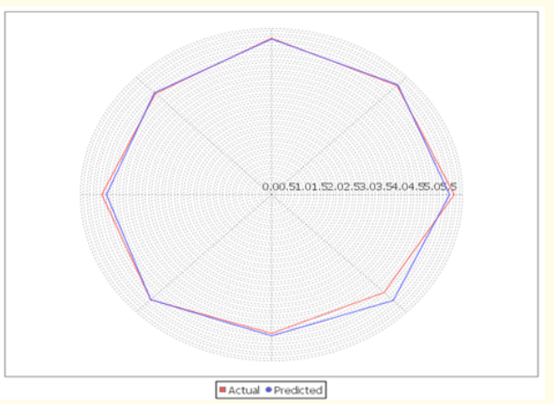

Figure 18: Actual and Predicted activity of training set by PLS method.

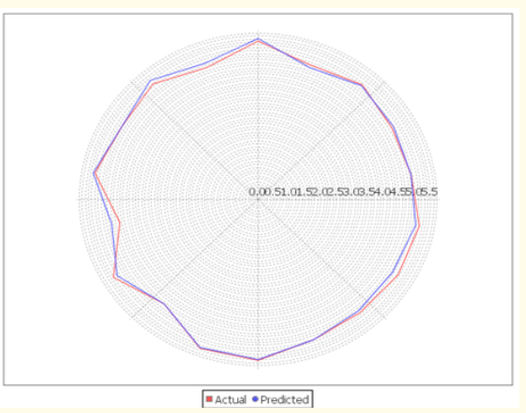

Figure 19: Actual and Predicted activity test set molecules by PLS method.

Stepwise (Forward)			
Descriptor	**Category**	**Contribution**	**Meaning**
SsOHE-index	Electrotopological	+	Number of –OH group connected with one single bond.
ZcompDipole	Semi-empirical	-	z component of the dipole moment
XAHydrophilicArea	Semi-empirical	-	vdW hydrophilic surface area.
XKMostHydrophobic HydrophilicDistance	Semi-empirical	+	Distance between most hydrophobic and hydrophilic point on the vdW surface.
SsOHE-index	Electrotopological	+	Number of –OH group connected with one single bond.
ZcompDipole	Semi-empirical	-	Signifies the z component of the dipole moment.
SssOcount	Topological	-	Total number of oxygen connected with two single bonds.
SAHydrophobicArea	Semi-empirical	+	Showing hydrophobic surface area.
SsOHE-index	Electrotopological	+	Number of –OH group connected with one single bond.
ZcompDipole	Semi-empirical	-	Signifies the z component of the dipole moment
chi4pathCluster	Topological	+	Signifies molecular connectivity index of 4th order path cluster.
SssOcount	Topological	-	Number of oxygen connected with two single bonds.

Table 14: Various descriptors obtained by various methods (MLR, PCR, PLS) under SW-F; their contributions and significance.

Stepwise (Forward-Backward)			
Descriptor	**Category**	**Contribution**	**Meaning**
SsOHE-index	Electrotopological	+	Number of –OH group connected with one single bond.
ZcompDipole	Semi-empirical	-	z component of the dipole moment
XAHydrophilicArea	Semi-empirical	-	vdW hydrophilic surface area.
XKMostHydrophobic HydrophilicDistance	Semi-empirical	+	Signifies distance between most hydrophobic and hydrophilic point on the vdW surface.
SsOHE-index	Electrotopological	+	Number of –OH group connected with one single bond.
ZcompDipole	Semi-empirical	-	Signifies the z component of the dipole moment.
SssOcount	Topological	-	Total number of oxygen connected with two single bonds.
SAHydrophobicArea	Semi-empirical	+	Showing hydrophobic surface area.
SsOHE-index	Electrotopological	+	Number of –OH group connected with one single bond.
ZcompDipole	Semi-empirical	-	Signifies the z component of the dipole moment
chi4pathCluster	Topological	+	Molecular connectivity index of 4th order path cluster.
SssOcount	Topological	-	Number of oxygen connected with two single bonds.

Table 15: Various descriptors obtained by various methods (PCR, MLR, PLS) under SW-FB; their contributions and significance.

In silico pharmacokinetic studies

ADME prediction

Number of the drugs under clinical trials could not see the clinics due to failure at the stage of pharmacokinetic evaluation. Initial screening of hits and leads before their clinical testing will not only decrease the rate of failure, but it reduces the cost of drugs discovery program. Taking into consideration, a preliminary predictive *in silico* pharmacokinetic study of the synthesized compounds was undertaken using online server preADMET (http://preadmet.bmdrc.org/). Incorporation of such tools as a part of the drug design process can screen molecules that are more likely to exhibit satisfactory absorption, distribution, metabolism, excretion (ADME) properties. The server calculated the parameters such as human intestinal absorption (HIA%), cellular permeability Caco-2 *in vitro*, cell permeability Maden Darby Canine Kidney (MDCK), plasma protein binding.

The results of ADME prediction are shown in table 16. These properties are presented as a determinant for drug development factors, being the biggest target objectives: good absorption, distribution, metabolism and excretion. Mainly, human intestinal absorption properties, because it is determinant for the drug development that purport to be administered orally. All the compounds under study presented human intestinal absorption value (HIA) in the range of 86.334 to 94.757. The absorption processes are related to the permeation of compounds through biological membrane under the influence of physicochemical characteristics, thus from present observation we can say that good physicochemical properties of the compounds enabled them to qualified HIA% with values > 70-100%.

Compound Name	HIA%	Caco-2 nm/sec	MDCK nm/sec	Plasma protein binding %
FN	93.071	26.327	0.76	90.982
Compound-7	94.757	20.939	0.048	90.830
Compound-8	86.334	12.266	0.044	94.846

Table 16: Pre-ADME prediction of ligands.

Further, the cell permeability *in vitro* Caco-2 is an important test to assess intestinal absorption of drugs. Since, Caco-2 cells derived from human colon adenocarcinoma, having various transport via in the intestinal epithelium. Table 16 is clearly indicating the cell permeability of the compounds **7, 8** and reference drug 26.327, whereas compound **8** with 12.266 could not meet the minimal requirement value of Caco-2 values (> 25 nm/sec) hence may get less permeation through human colon adenocarcinoma.

On the other hand, MDCK system utilizes canine kidney cells and has a shorter growth that the Caco-2 cells. Thus, this system is used as a tool for the rapid analysis of permeability. Reported methods states that the permeability can be classified into low (< 25 nm/sec) and mean (> 25 to 500 nm/sec). Further, analyzing the data in this MDCK system of the various inhibitors, present value in table 16 indicates that the compound **7** and **8** have low permeability towards kidney cells with values ranging from 0.044 nm/sec to 0.048 nm/sec respectively.

The drug has two forms in the blood, the plasma protein bond form and non-bond form, although that bond directly depends on their affinity for such bond portion and the free portion. The binding to these proteins can alter the half-life of the drug in the body of the individual. Distribution properties of plasma protein binding (PPB%) in table 16, indicated that both the compounds binds strongly to plasma proteins i.e. (> 90%). In addition to changing the pharmacological response of molecules, the PPB also modifies the renal excretion because only unbound drug is available for glomerular filtration thus increasing excretion and decreasing half-life.

Conclusion

Compounds **7, 8** were synthesised in bulk quantities for their characterization and physicochemical properties determination. Pure crystalline nature of compound **7** and **8** was confirmed by single endothermic peak in DSC. PXRD studies indicated the more crystalline nature of compound 8 in comparison to compound **7**, which was further supported by its lesser solubility and more enthalpy of solution in all different mediums as compared compound **8**. The maximum solubility was found in water and 0.1 N HCl (pH 1.6) indicated the affinity of the synthesized compounds for aqueous compartments or acidic medium. The acid/base character sets the charge of a molecule in solution at a particular pH. It can be described by the protonation constant (logK). Pka value of the newly synthesized and evaluated compounds are in the range of 5.56- 8, closer to reference drug Finasteride with pka 6.63, that indicated their weak basic nature. Compounds with pka in range of 5-11 are weak bases and are found to possess good or high absorption in intestine. Results of dissolution studies with better dissolution in medium with acidic pH 1.6 are in concordance with their respective pKa values. The logarithm of octanol/water partition coefficient (log P Oct) is the most extensively used parameter in medicinal chemistry to quantitative lipophilicity and has been found to be a good predictor of the passive transport of drugs through the lipoid membranes of the human body. Observed partition coefficient values for the compound **7** and **8** in the range of 3 - 4, are in accordance with Lipinski rule of five, further indicated their good permeability. Also predicted log p has been found to parallel with experimentally determined values. This agreement between computation and experiment results lends support to the reliability and accuracy to results achieved in this study. Earlier published report has indicated the highest antiproliferative activity of the compound **7**, which can be attributed to its log p with better permeability, better solubility, higher dissolution rate. 2D QSAR model was developed using published data from our laboratory, and used to predict the activity of synthesized compounds. Residual value i.e. difference in the observed and predicted activity is which were in concordance with experimental values. QSAR models were statistically significant, but results obtained for the present series of 3β-substituted esters of 17 lactam, 17-oxo, 17-oximino androstane derivatives showed good correlation as manifested from the best model 1 (r^2 = 0.833, q^2 = 0.6711; F = 37.498, pred r^2 = 0.736) with human 5α-reductase inhibitory activity. The prediction power of the QSAR model was tested by LOO method, which gives a good internal predictivity. QSAR study indicated the influence of various physicochemical parameters, including SssOcount (negative), ZcompDipole (negative), SssOcount (negative), XKMostHydrophobicHydrophilicDistance (negative), XlogP (positive), chi4pathCluster) (positive), (negative), SsNH2count (positive), XAHydrophilicArea (positive) and many other descriptors used against human 5α-reductase. These results will be helpful in designing new structural human 5α-reductase inhibitors as agents for the treatment of BPH. An estimation of the post synthesis preliminary physicochemical profiling in terms of solubility, dissolution rates, pKa and permeability (logP) has not only added to enhance the bank information on the synthesized highly significant molecules, but provided an overview of their bioperformance, and facilitated decision making during lead optimization. Results obtained from these studies shall be used as guidelines for further development of novel compounds to be used in the pharmacotherapy for BPH.

Conflict of Interest

The authors confirm that this article content has no conflict of interest.

Acknowledgment

The authors are thankful to the Dr Amit Bedi, and Dr Kundan; Vlife Science Technologies Pvt. Ltd, Pune, India, for providing us with the VlifeMDS 4.3 software and for their continual support in the QSAR study. The grants received from Department of Science and Technology (DST), are gratefully acknowledged.

Bibliography

1. Aggarwal Saurabh., *et al.* "An overview on 5α-reductase inhibitors". *Steroids* 75.2 (2010): 109-153.

2. Dhingra Neelima and Deepak Bhagwat. "Benign prostatic hyperplasia: An overview of existing treatment". *Indian Journal of Pharmacology* 43.1 (2011): 6-12.

3. Ziada Ali Mark Rosenblum and E David Crawford. "Benign prostatic hyperplasia: an overview". *Urology* 53.3 (1999): 1-6.

4. Griffiths Derek J. "Pressure-flow studies of micturition". *Urologic Clinics* 23.2 (1996): 279-297.

5. Celotti Fabio., *et al.* "Steroid metabolism in the mammalian brain: 5alpha-reduction and aromatization". *Brain Research Bulletin* 44.4 (1997): 365-375.

6. Weisser Heike and M Krieg. "Benign prostatic hyperplasia--the outcome of age-induced alteration of androgen-estrogen balance?" *Der Urologe* 36.1 (1997): 3-9.

7. Lee Chung James., *et al.* "Etiology of benign prostatic hyperplasia". *The Urologic Clinics of North America* 22.2 (1995): 237-246.

8. Thorpe A and D Neal. "Benign prostatic hyperplasia". *The Lancet* 361.9366 (2003): 1359-1367.

9. Beduschi Mario C., *et al.* "Alpha-blockade therapy for benign prostatic hyperplasia: from a nonselective to a more selective alpha 1A-adrenergic antagonist". *Urology* 51.6 (1998): 861-872.

10. Eri Lars M and Kjell J Tveter. "Treatment of Benign Prostatic Hyperplasia". *Drugs and Aging* 10.2 (1997): 107-118.

11. Wilson Jean D. "Sexual differentiation of the gonads and of the reproductive tract". *Neonatology* 55.6 (1989): 322-330.

12. Teilum Gunnar. "Classification of testicular and ovarian androblastoma and Sertoli cell tumors. A survey of comparative studies with consideration of histogenesis, endocrinology, and embryological theories". *Cancer* 11.4 (1958): 769-782.

13. Schroder F H. "Steroid Receptors, Metabolism and Prostatic Cancer". Proceedings of a Workshop of the Society, Amsterdam, Excerpta Medica (1980).

14. Jenkins E P., *et al.* "Genetic and pharmacological evidence for more than one human steroid 5 alpha-reductase". *Journal of Clinical Investigation* 89.1 (1992): 293.

15. Russell David W and Jean D Wilson. "Steroid 5alpha-reductase: two genes/two enzymes". *Annual review of biochemistry* 63.1 (1994): 25-61.

16. Glina Sidney., *et al*. "Sexual Function in Men with Lower Urinary Tract Symptoms and Prostatic Enlargement Secondary to Benign Prostatic Hyperplasia: Results of a 6-Month, Randomized, Double-Blind, Placebo-Controlled Study of Tadalafil Coadministered with Finasteride". *The Journal of Sexual Medicine* 12.1 (2015): 129-138.

17. Iehlé Catherine., *et al.* "Human prostatic steroid 5α-reductase isoforms-A comparative study of selective inhibitors". *The Journal of Steroid Biochemistry and Molecular Biology* 54.5 (1995): 273-279.

18. Serafini Paulo and Rogerio A Lobo. "Increased 5α-reductase activity in idiopathic hirsutism". *Fertility and Sterility* 43.1 (1985): 74-78.

19. Brooks J R. "12 Treatment of hirsutism with 5α-reductase inhibitors". *Clinics in Endocrinology and Metabolism* 15.2 (1986): 391-405.

20. Bingham K D and D A Shaw. "The metabolism of testosterone by human male scalp skin". *Journal of Endocrinology* 57.1 (1973): 111-121.

21. Berardinelli F., *et al.* "Minimally invasive surgery in the management of benign prostatic hyperplasia". *Minerva urologica e nefrologica= The Italian Journal of Urology and Nephrology* 61.3 (2009): 269-289.

22. Tanguay Simon., *et al.* "Diagnosis and management of benign prostatic hyperplasia in primary care". *Canadian Urological Association Journal* 3.3 (2009): S92.

23. Krieg Michael., *et al.* "Androgens and estrogens: their interaction with stroma and epithelium of human benign prostatic hyperplasia and normal prostate". *Journal of Steroid Biochemistry* 19.1 (1983): 155-161.

24. Frick J. "Pathophysiology of benign prostatic hyperplasia". *Wiener medizinische Wochenschrift (1946)* 146.8 (1996): 158-160.

25. Blohm T R., *et al.* "Pharmacological induction of 5 α-reductase deficiency in the rat: separation of testosterone-mediated and 5 α-dihydrotestosterone-mediated effects". *Endocrinology* 119.3 (1986): 959-966.

26. Jønler Morten., *et al.* "Benign prostatic hyperplasia". *Drugs* 47.1 (1994): 66-81.

27. Scott W W and J C Wade. "Medical treatment of benign nodular prostatic hyperplasia with cyproterone acetate". *The Journal of Urology* 101.1 (1969): 81.

28. Guess H A., *et al.* "The effect of finasteride on prostate-specific antigen in men with benign prostatic hyperplasia". *The Prostate* 22.1 (1993): 31-37.

29. Holt Dennis A., *et al.* "Inhibition of steroid 5. alpha. -reductase by unsaturated 3-carboxy steroids". *Journal of Medicinal Chemistry* 33.3 (1990): 943-950.

30. Ibrahim-Ouali Malika and Luc Rocheblave. "Recent advances in azasteroids chemistry". *Steroids* 73.4 (2008): 375-407.

31. Huang Yanmin., *et al.* "Synthesis and evaluation of some new aza-B-homocholestane derivatives as anticancer agents". *Marine Drugs* 12.4 (2014): 1715-1731.

32. Occhiato Ernesto G*., et al.* "Selective non-steroidal inhibitors of 5α-reductase type 1". *The Journal of Steroid Biochemistry and Molecular Biology* 88.1 (2004): 1-16.

33. Ibrahim-Ouali Malika. "Total synthesis of steroids and heterosteroids from BISTRO". *Steroids* 98 (2015): 9-28.

34. Singh Harkishan*., et al.* "2 Heterosteroids and Drug Research". *Progress in Medicinal Chemistry* 16 (1979): 35-149.

35. Martin-Smith M and M F Sugrue. "Biological activity in steroids possessing nitrogen atoms: recent advances". *Journal of Pharmacy and Pharmacology* 16.9 (1964): 569-595.

36. Chen Jiyun*., et al.* "Discovery and therapeutic promise of selective androgen receptor modulators". *Molecular Interventions* 5.3 (2005): 173-188.

37. Rasmusson Gary H., *et al*. "N-monosubstituted adamantyl/norbornanyl 17β-carbamides of 3-carboxy-androst-3, 5-dienes as testosterone 5α-reductase inhibitors". U.S (1992).

38. Kim Sujeong*., et al.* "Synthesis and 5α-reductase inhibitory activity of C21 steroids having 1, 4-diene or 4, 6-diene 20-ones and 4-azasteroid 20-oximes". *Molecules* 17.1 (2011): 355-368.

39. Holt Dennis A., *et al.* "Steroidal A ring aryl carboxylic acids: a new class of steroid 5. alpha. -reductase inhibitors". *Journal of Medicinal Chemistry* 33.3 (1990): 937-942.

40. Liang Tehming*, et al*. "4-Azasteroidal 5 alpha-reductase inhibitors without affinity for the androgen receptor". *Journal of Biological Chemistry* 259.2 (1984): 734-739.

41. Azzolina B., *et al*. "Inhibition of rat α-reductases by finasteride: evidence for isozyme differences in the mechanism of inhibition". *The Journal of Steroid Biochemistry and Molecular Biology* 61.1 (1997): 55-64.

42. Rasmusson Gary H*., et al.* "Azasteroids as inhibitors of rat prostatic 5. alpha. -reductase". *Journal of Medicinal Chemistry* 27.12 (1984): 1690-1701.

43. Rasmusson Gary H., *et al*. "Azasteroids: structure-activity relationships for inhibition of 5 alpha. -reductase and of androgen receptor binding". *Journal of Medicinal Chemistry* 29.11 (1986): 2298-2315.

44. Levy Mark A., *et al*. "Inhibition of rat liver steroid 5. alpha. -reductase by 3-androstene-3-carboxylic acids: mechanism of enzyme-inhibitor interaction". *Biochemistry* 29.11 (1990): 2815-2824.

45. Rasmusson Gary H., *et al*. "17β-acyl-3-carboxy-androsta-3, 5-dienes as testosterone 5α-reductase inhibitors". U.S (1993).

46. Malhotra Manav., *et al.* "17-Aza Steroids as 5α-Reductase Inhibitors: A Review". *International Journal of Pharmacognosy and Phytochemical Research* 5.2 (2013): 134-142.

47. Cabeza Marisa., *et al.* "New progesterone esters as 5α-reductase inhibitors". *Chemical and Pharmaceutical Bulletin* 49.9 (2001): 1081-1084.

48. Dhingra Neelima., *et al.* "Synthesis, antiproliferative activity, acute toxicity and assessment of the antiandrogenic activities of new androstane derivatives". *Archives of Pharmacal Research* 34.7 (2011): 1055-1063.

49. Wang Cunde*., et al.* "Preparation of (5α, 13α)-d-azasteroids as key precursors of a new family of potential GABA A receptor modulators". *Steroids* 68.7 (2003): 677-683.

50. McDonald Ian A., *et al.* "Inhibition of steroid 5α-reductase by "inverted", competitive inhibitors". *Bioorganic and Medicinal Chemistry Letters* 4.6 (1994): 847-851.

51. Gupta R., *et al*. "Synthesis and biological activity of azasteroidal 3, 2-c.-and 17, 16-c. pyrazoles". *European Journal of Medicinal Chemistry* 31.3 (1996): 241-247.

52. Metcalf Brian W., *et al*. "Potent inhibition of human steroid 5α-reductase (EC 1.3. 1.30) by 3-androstene-3-carboxylic acids". *Bioorganic Chemistry* 17.3 (1989): 372-376.

53. Pinto-Bazurco Mendieta., *et al.* "Synthesis, biological evaluation, and molecular modeling of abiraterone analogues: novel CYP17 inhibitors for the treatment of prostate cancer". *Journal of Medicinal Chemistry* 51.16 (2008): 5009-5018.

54. Guha Rajarshi and Peter C Jurs. "Development of QSAR models to predict and interpret the biological activity of artemisinin analogues". *Journal of Chemical Information and Computer Sciences* 44.4 (2004): 1440-1449.

55. Roy, Kunal, Supratik Kar and Rudra Narayan Das. "A primer on QSAR/QSPR modeling: Fundamental concepts". Springer (2015).

56. Dhingra Neelima, *et al.* "17-Oximino-5-androsten-3β-yl esters: synthesis, antiproliferative activity, acute toxicity, and effect on serum androgen level". *Medicinal Chemistry Research* 20.7 (2011): 817-825.

57. Offerdahl Thomas J*., et al.* "Quantitation of crystalline and amorphous forms of anhydrous neotame using 13C CPMAS NMR spectroscopy". *Journal of Pharmaceutical Sciences* 94.12 (2005): 2591-2605.

58. Santos Olimpia Maria Martins., *et al*. "A dissolution test for finasteride in immediate-release capsules". *Dissolution Technologies* 20.3 (2013): 25-34.

59. Reijenga Jetse., *et al.* "Development of methods for the determination of pKa values". *Analytical Chemistry Insights* 8 (2013): 53-71.

60. Okur Neslihan Üstündağ., *et al*. "Evaluation of skin permeation and anti-inflammatory and analgesic effects of new naproxen microemulsion formulations". *International Journal of Pharmaceutics* 416.1 (2011): 136-144.

61. Sirisoma Nilantha., *et al.* "Discovery of N-methyl-4-(4-methoxyanilino) quinazolines as potent apoptosis inducers. Structure–activity relationship of the quinazoline ring". *Bioorganic and Medicinal Chemistry Letters* 20.7 (2010): 2330-2334.

62. Mosmann Tim. "Rapid colorimetric assay for cellular growth and survival: application to proliferation and cytotoxicity assays". *Journal of Immunological Methods* 65.1-2 (1983): 55-63.

63. Noolvi Malleshappa N and Harun M Patel. "A comparative QSAR analysis and molecular docking studies of quinazoline derivatives as tyrosine kinase (EGFR) inhibitors: A rational approach to anticancer drug design". *Journal of Saudi Chemical Society* 17.4 (2013): 361-379.

64. Croux Christophe and Kristel Joossens. "Influence of observations on the misclassification probability in quadratic discriminant analysis". *Journal of Multivariate Analysis* 96.2 (2005): 384-403.

65. Devillers James. "Neural networks in QSAR and drug design". Academic Press (1996).

66. Heckler Charles E. "Applied Discriminant Analysis". *Technometrics* 37.3 (1995): 349-350.

67. Doucet Jean-Pierre., *et al.* "Nonlinear SVM approaches to QSPR/QSAR studies and drug design". *Current Computer-Aided Drug Design* 3.4 (2007): 263-289.

68. Mason Harold L and Edwin J Kepler. "Isolation of steroids from the urine of patients with adrenal cortical tumors and adrenal cortical hyperplasia: A new 17-ketosteroid, androstane-3 (α), 11-diol-17-one". *Journal of Biological Chemistry* 161.1 (1945): 235-257.

69. Silva Nayara SR., *et al.* "Computational analysis of physicochemical, pharmacokinetic and toxicological properties of deoxyhypusine synthase inhibitors with antimalarial activity". *Computational Molecular Bioscience* 4.04 (2014): 47-57.

70. Hershberg E B. "Regeneration Of Steroid Ketones From Their Semicarbazones With Pyruvic Acid1". *The Journal of Organic Chemistry* 13.4 (1948): 542-546.

71. Regan Bernard M and F Newton Hayes. "17-and 17a-Aza-D-homosteroids1, 2". *Journal of the American Chemical Society* 78.3 (1956): 639-643.

72. Smith Michael B and Jerry March. "March's advanced organic chemistry: reactions, mechanisms, and structure". *John Wiley & Sons* (2007).

73. Rogers David and Anton J Hopfinger. "Application of genetic function approximation to quantitative structure-activity relationships and quantitative structure-property relationships". *Journal of Chemical Information and Computer Sciences* 34.4 (1994): 854-866.

74. Khamis Harry J. "The δ-corrected kolmogorov-smirnov test for goodness of fit". *Journal of Statistical Planning and Inference* 24.3 (1990): 317-335.

75. Byvatov Evgeny and Gisbert Schneider. "SVM-based feature selection for characterization of focused compound collections". *Journal of Chemical Information and Computer Sciences* 44.3 (2004): 993-999.

76. Kirkpatrick Scott C., et al. "Optimization by simulated annealing". *Science* 220.4598 (1983): 671-680.

77. Agrafiotis Dimitris K. "Stochastic algorithms for maximizing molecular diversity". *Journal of Chemical Information and Computer Sciences* 37.5 (1997): 841-851.

78. Seierstad Mark and Dimitris K Agrafiotis. "A QSAR model of hERG binding using a large, diverse, and internally consistent training set". *Chemical Biology and Drug Design* 67.4 (2006): 284-296.

Volume 2 Issue 2 February 2018